DEVELOPMENT OF TiO_2/ACTIVATED CARBON COMPOSITE PHOTOCATALYST FOR THE REMOVAL OF METHANOL AND HYDROGEN SULFIDE FROM PAPER MILLS

By

YONG TAO

A DISSERTATION PRESENTED TO THE GRADUATE SCHOOL
OF THE UNIVERSITY OF FLORIDA IN PARTIAL FULFILLMENT
OF THE REQUIREMENTS FOR THE DEGREE OF
DOCTOR OF PHILOSOPHY

UNIVERSITY OF FLORIDA

2006

To my parents, Bang-He Tao and Ping-Fen Li, who raised me up. Your love is always in my heart. To my twin sister, Hui Tao. Without your encouragement and support, I could not have this achievement.

ACKNOWLEDGMENTS

I would like to give my sincere gratitude to Dr. Chang-Yu Wu for his support and guidance in my Ph.D. study. His advice and encouragement were precious for my graduate study. My special thanks go to my committee, Dr. David W. Mazyck, Dr. Jean M. Andino, and Dr. Wolfgang Sigmund, who gave me continuous comments and valuable advice on my research.

I also thank the staff in ERC and MAIC for teaching and allowing me to use many instruments such as XRD, SEM, and BET. I would like to thank our past and present group members. Special thanks go to Jennifer, Ameena, Yu-Mei, A-Chuan, Ying, and Anadi.

Finally I would like to give my sincere gratitude to my family. Without their care and encouragement, I could not have achieved this goal.

TABLE OF CONTENTS

LIST OF TABLES

LIST OF FIGURES

Abstract of Dissertation Presented to the Graduate School
of the University of Florida in Partial Fulfillment of the
Requirements for the Degree of Doctor of Philosophy

DEVELOPMENT OF TiO_2/ACTIVATED CARBON COMPOSITE PHOTOCATALYST FOR THE REMOVAL OF METHANOL AND HYDROGEN SULFIDE FROM PAPER MILLS

By

Yong Tao

May, 2006

Chair: Chang-Yu Wu
Major Department: Environmental Engineering Sciences

The objective of this study was to investigate the technical efficacy of in-situ treatment of pulp and paper emissions via adsorption and photocatalytic regeneration.

Firstly, activated carbon was coated with a commercially available photocatalyst by a spray desiccation method. The spent TiO_2/AC was regenerated by UV light irradiation. The photocatalytic regeneration is ascribed to both desorption from AC and photocatalytic degradation on TiO_2.

In order to improve the photocatalytic degradation rate, the synthesis of TiO_2/AC composites by dry impregnation method was developed. The composites prepared using various hydrolysis and calcination conditions were evaluated. High hydrolysis temperature resulted in rough particulate coating layers with higher surface area. The TiO_2 loading was positively correlated with the precursor concentration although the TiO_2 loading in the study range (2 – 8 wt%) was not critical to the photocatalytic

performance. The moisture in carbon was beneficial for the hydrolysis of precursor (titanium tetra-isopropoxide, TTIP) and improved the composite performance. Under proper preparation conditions, the TiO_2/AC composite outperformed the composite prepared by spray desiccation at removing methanol.

The BioNuchar AC support itself was a good H_2S remover. After coating TiO_2 by dry impregnation, H_2S removal efficiency of TiO_2/AC decreased compared with the virgin AC due to the change of surface pH. Under UV light irradiation, H_2S removal efficiency of TiO_2/AC composite doubled, and its sulfate conversion efficiency was higher than that of AC. The formation of sulfate is preferred for water regeneration.

TiO_2/AC composite photocatalyst was also prepared by a novel microwave-assisted impregnation method and was employed for the removal of methanol from humid air streams. A commercial microwave oven (800 W) was used as the microwave source. Under 2450 MHz microwave irradiation, TTIP was quickly hydrolyzed and anatase TiO_2 was formed in a short time (< 20 minutes). Due to the volumetric heating and selective heating of microwave, the solvent and by-products were quickly removed which reduced energy consumption and processing time. The formed submicron TiO_2 particles were mainly deposited on the external surface of carbon and had photocatalytic activity.

CHAPTER 1
GENERAL INTRODUCTION

The pulp and paper industry deserves special attention for both its energy and environmental impact. It is the fourth largest consumer of electricity and fuels and the third largest consumer of fresh water in the United States (Sittig, 1977). During the 4 years spanning 1997-2000, the pulp and paper industry spent $6 billion per year on energy, or about 4 percent of its net sales and averaged over $800 million per year on environmental protection capital, or about 14 percent of the average annual capital invested on equipment (Department of Energy [DOE], 2003).

To produce paper or paperboard, the wood is pulped at first. Pulps are made from wood chips, whole tree chips, sawmill residues, or logs. Pulps can be prepared through chemical and/or mechanical means. The pulp may then be bleached to various degrees of brightness. Finally, bleached or unbleached pulp is processed into paper board or paper. The dominant wood pulping process today is the Kraft process (Buonicore and Davis, 1992). Figure 1-1 shows a simplified process flow sheet of the pulp mill (Buonicore and Davis, 1992).

Pulp and paper mill effluents are complex mixtures. The characteristics of each effluent are dependent on numerous factors including wood furnish and process technology (including washing, cooking, bleaching, prebleaching, etc.), as well as final effluent treatment (Serros, 1996). The atmospheric emissions from the Kraft process include both gaseous and particulate materials. The major gaseous emissions are malodorous reduced sulfur compounds referred to as total reduced sulfur (TRS), such as

hydrogen sulfide (H_2S), methyl mercaptan (CH_3SH), dimethyl sulfide ($(CH_3)_2S$), and dimethyl disulfide ($(CH_3)_2S_2$); organic nonsulfur compounds; oxides of sulfur; and oxides of nitrogen . The particulate emissions are primarily sodium sulfate and sodium carbonate. Historically, odor and visible particulate emissions from Kraft pulp mills have received considerable attention. A summary of the major control techniques for gaseous and particulate emissions from specific kraft pulp mill sources are presented in Table 1-1.

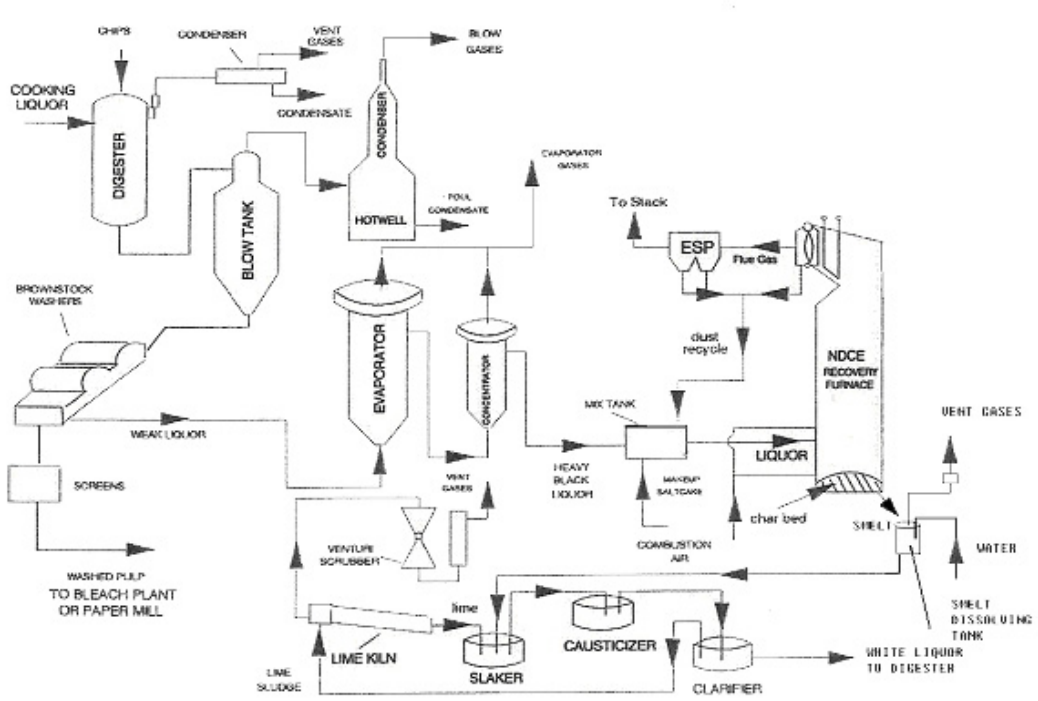

Figure 1-1 Simplified process flow chart of the Kraft pulp mill (adapted from Buonicore and Davis, 1992)

In 1992, the National Council of the Paper Industry Air and Stream Improvement, Inc. (NCASI) conducted a study to characterize the emissions of volatile organic compounds (VOCs) and hazardous air pollutants (HAPs) from chemical pulp mill sources (NCASI, 1994). Seven lime kilns, four smelt dissolving tanks, and a number of

Table 1-1 Pollution control techniques for gaseous and particulate matter emissions from Kraft pulp mill sources

Emission Source	Gaseous Control	Particulate Control
Digester gases	Incineration Condensation	NA(not applicable)
Washer vent	Incineration	NA
Evaporator gases	Incineration Scrubbing Condensation	NA
Condensate water	Steam stripping Air stripping	NA
Condensate Stripper Vent	Incineration	NA
Black Liquor Oxidation Tower Vent	Incineration	NA
Tall Oil Vent	Scrubbing	NA
Recovery Furnance	Scrubbing	Precipitators Scrubbing
Smelt Tank	Scrubbing	Scrubbing
Lime Kiln	Scrubbing	Precipitators Scrubbing
Slaker Vent	NA	Scrubbing
Bleach Plant	Scrubbing	NA
Paper Machine	Incineration Adsorption Condensation	NA
Power Boiler	NA	Cyclones Precipitators Scrubbing

(Adapted from Sittig, 1996)

vents in the causticizing areas of eight mills were tested. Their results showed the average HAPs and EPA method 25A VOC emissions from causticizing areas vents, including lime kilns, smelt dissolving tanks, and miscellaneous causticizing area vents, were 0.66 lb/ADTP (pounds/air dried tons of pulp) and 0.48 lb C/ADTP (lb as carbon (Method 25 A)/ADTP). The smelt dissolving tank contributed over 75% of the total HAP emissions. The total HAP emissions of the four tested smelt dissolving tank scrubbers vent averaged 0.50 lb C/ADTP, and methanol was the major HAP which contributed on average 98% to the total HAPs. The average concentration of methanol in the four tested smelt dissolving

tank scrubbers' vent ranged from around 10 to 1100 ppm. The flow rates ranged from 5000 to 16000 DSCFM (dry standard cubic feet per minute).

Although odor emissions from pulp and paper mill have received considerable attention, the control and abatement of them are difficult tasks to achieve in the air pollution problems afflicting the paper and pulp mills. This is due to the very low human olfactory threshold levels of TRS gases. Two main TRS sources are recognized to occur in paper and pulp mills: 1) the LVHC (low volume high concentration) gases, usually dealt with by incineration, emerge from brownstock washers, digester, and evaporator systems, etc.; 2) the HVLC (high volume low concentration) gases, dealt with by alkaline amine wet scrubbing, are released by recovery furnaces and lime kilns. However, these control devices can not remove all the pollutants. Bordado and Gomes (2001) characterized the reduced sulfur compounds emitted from a Kraft pulp mill, which was the biggest Portuguese plant producing bleached eucalyptus elemental chlorine free pulp and its output was 430,000 t/yr. Table 1-2 shows part of their results (Bordado and Gomes, 2001). It is clear that there is considerable amount of TRS gases in the emissions from incinerators and scrubbers.

In 1998, the U.S. Environmental Protection Agency (EPA) promulgated the "cluster rules" for the pulp and paper industry. The Maximum Achievable Control Technology (MACT) portion of the April 1998 Cluster Rule specifies the control of hazardous air pollutant emissions. For the pulp and paper industry, this is primarily methanol. These rules require compliance by April 15, 2001. Additional controls will be required by 2006 for HVLC streams (Springer, 2000). New regulations for air emission have stimulated researchers to search for a coat-effective technique for in-situ treatment

of these pollutants. A limited number of Kraft mills currently have HVLC collection and incineration systems in place (Varma, 2003). Considering the operating cost and the formation of noxious by-products, incineration is unfavorable in the long run. Therefore, an alternative technique for the treatment of the HVLC emission is worthy of exploration.

Table 1-2 H_2S and total reduced sulfur (TRS) compounds emissions

source	H_2S		Q	H_2S Emission	TRS Emission
	(ppm)	(mg/Nm^3)	(m^3/h)	(kg/h)	(kg/h)
Stationary sources					
Recovery boiler scrubber	<5	<7.2	183100	<1.318	16.5
Smelt tank	70	100.8	5000	0.504	0.754
Incinerator exhaust	<5	<7.2	5000	<0.036	0.679
Incinerator scrubber	48	69.12	5000	0.346	0.346
Lime kiln	17	24.48	21200	0.519	0.519
Pulp cooking and Washing section					
Bin hopper	46	66.24	3900	0.258	7.793
Pulp bleaching section					
Oxygen reactor	<5	<7.2	2662.9	<0.019	0.24

(Adapted Bordado and Davis, 2001)

Granular activated carbon (GAC) adsorption is a commonly used technique for the removal of various VOCs and HAPs. The major limitation of activated carbon adsorption is its nondestructive character. Once exhausted, activated carbon is either disposed of, or treated to destroy the adsorbed pollutants (regeneration). Moreover, the spent carbon itself may have to be handled as a hazardous waste when disposed of (Liu et al., 1996). Regeneration of spent carbon is a very critical step to the effective use of carbon and thus lowers the cost.

Recently, heterogeneous photocatalysis and its application in environmental cleanup have been one of the most active research topics. Scientific research in heterogeneous photocatalysis started in 1970s. Fujishima and Honda (1972) discovered the photocatalytic splitting of water on TiO_2 electrodes, which marked the beginning of a

new era in heterogeneous photocatalysis. Photocatalysts are invariably semiconductors, which can promote reactions in the presence of light and are not consumed in the overall reactions. Nanosized titanium dioxide (TiO_2) under the form of anatase has been found as an excellent photocatalyst since it is able to utilize near UV light, is safe, and is inexpensive. It has been shown to be effective for a variety of inorganic and organic compounds, for the destruction of microorganisms, for the inactivation of cancer cells, for odor control, and for the clean-up of oil spills. (Hoffmann et al., 1995; Linsebigler et al., 1995; Peral et al., 1997; Bhatkhande et al., 2001)

Figure 1-2 shows the mechanism of photocatalysis. Semiconductors possess a void energy region, which extends from the top of the filled valence band (VB) to the bottom of the vacant conduction band (CB). This void region is called band gap. By light absorption with energy equal to or greater than the band gap, an electron in the VB is excited to the CB (the enlarged section of Figure 1-2). The highly reactive electron-hole pair undergoes de-excitations in several pathways, as shown in Figure 1-2. A photoinduced electron can migrate to the surface and reduce the electron acceptor (usually oxygen in air or an aerated solution). A photoinduced hole can migrate to the surface and oxidize the donor species. In this way, highly reactive radical species, such as hydroxyl radical OH• and superoxdie ion O_2^- , are formed. Pollutant degradation may occur indirectly via the surface-bound hydroxyl radical or directly via the VB hole before it is trapped (Hoffmann et al., 1995; Linsebigler et al., 1995; Peral et al., 1997; Bhatkhande et al., 2001).

In practice, the separation of nanosized photocatalyst from the treated fluid limits its industrial applicability (Chen et al., 2001; El-Sheikh et al., 2004). To overcome this

drawback, the powder photocatalyst can be dispersed onto a support. The photocatalyst coated on nonporous support has a limited contact area, thus low efficiency (El-Sheikh et al., 2004). Porous support has been used to enhance the efficiency (El-Sheikh et al., 2004). Activated carbon is chemically inert at low temperature and hence is a suitable support for photocatalysts (Torimoto et al., 1997; Harada et al., 1999; Khan, 2003;Tao et al., 2005).

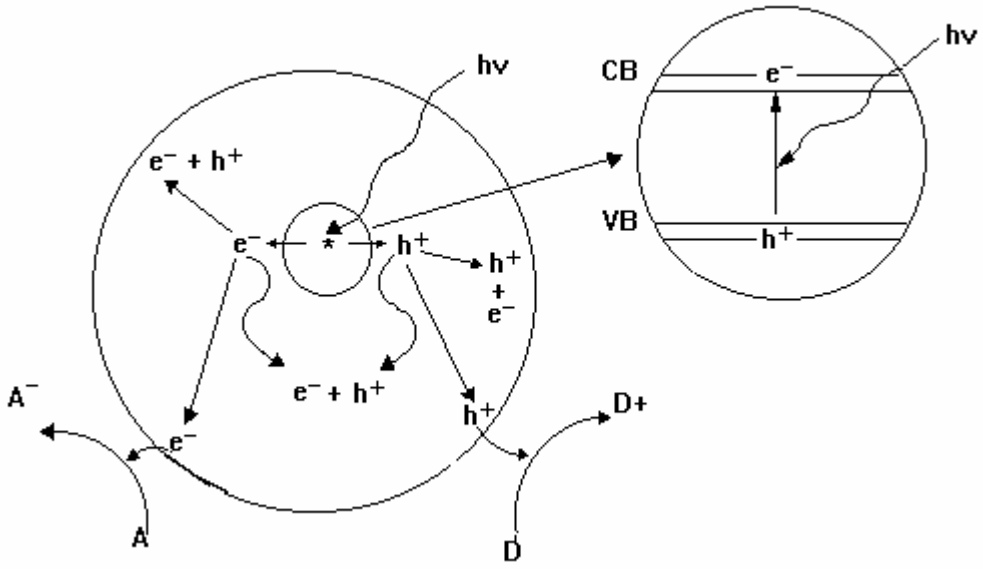

Figure 1-2 Schematic photoexcitation in a photocatalyst followed by deexciatation events. (Linsebigler et al., 1995)

On the other hand, in a heterogeneous photocatalysis system, photoinduced molecular transformations take place at the surface of a catalyst (Linsebigler et al., 1995). The destruction rate is dependent upon the ability of the pollutants to diffuse to the catalyst. When the pollutants' concentrations are low, the degradation rates are low. Malato and coworkers (2001) studied the photocatalytic oxidation of *2,4*-Dichlorophenol (DCP) in water using Degussa P25 TiO_2 (BET specific surface area ≈ 50 $m^2 g^{-1}$, mean primary particle diameter ≈ 20 nm, density = 4 g cm^{-3}, 80% anatase phase/20% rutile

phase) suspension under solar radiation. Their result showed that mineralization of DCP was slow when its concentration was low. They proposed a combination of photocatalytic degradation with granular AC treatment. The effluent from the photocatalytic process was filtered through a granular AC adsorber. The total cost was reduced considerably by using AC adsorption as the last step of treatment (Malato et al., 2001). However, the saturated AC must be disposed of or regenerated.

Immobilizing TiO_2 on AC can result in a synergistic combination of both adsorption and photocatalysis. On one hand, AC works as the support of nanosized TiO_2 photocatalyst and concentrates the pollutants and intermediates around the TiO_2; on the other hand, the photocatalyst can destroy the pollutants thus regenerating the AC in situ. In traditional thermal or microwave regeneration, part of the pollutants is simply desorbed. Regeneration on the TiO_2/AC composite is achieved by photocatalytic oxidation of pollutants; thus no post-treatment is needed for the desorbed pollutants. Besides the advantage of low-temperature in situ regeneration, this novel composite possesses synergistic functions of simultaneous adsorption and oxidation that are greater than in the cases when either carbon or TiO_2 irradiated with ultraviolet (UV) light is employed alone (Herrmann and Guillard, 2000; Matos et al., 2001; Khan, 2003).

In summary, the TiO_2/AC composite photocatalyst for air pollution control of pulp and paper mills is a technique worthy of exploration. In Chapter 2, the technical efficacy of photocatalytic regeneration was studied. Methanol was chosen as the model pollutant. The effects of humidity and purge air on regeneration were investigated. In Chapter 3, a dry impregnation method was developed to prepare TiO_2/AC composite photocatalyst in order to improve its performance. The impacts of preparation conditions on the

photocatalytic activity (methanol as the model pollutant) of prepared TiO_2/AC were further studied. In Chapter 4, the removal performance of hydrogen sulfide, which was chosen as the representative of TRS gases, was tested. In Chapter 5, a novel microwave-assisted impregnation was developed to prepare TiO_2/AC composite photocatalyst. In Chapter 6, conclusion of this work and recommendations are provided.

CHAPTER 2
PHOTOCATALYTIC REGENERATION

Introduction

One of the major technologies for the abatement of low concentrations of toxic organic compounds in air is adsorption. Activated carbon (AC) is by far the most frequently used adsorbent. The term "activated" refers to the increased internal and external surface area imparted by special treatment processes. Any carbonaceous materials, such as coconut shells, bones, wood, coal, petroleum coke, lignin, and lignite, can be converted to AC. AC is manufactured by first dehydrating and carbonizing the carbonaceous raw material. Activation is completed by heating the carbonized materials in the presence of an oxidizing gas (usually CO_2 or H_2O) during a controlled oxidation step. AC is tailored for special end use by both raw material selection and control of the activation process. ACs typically have a surface area in the range from 600 to 1400 m^2/g, an internal porosity from 55% to 75%. Most of the pore volume is distributed over a narrow range of pore diameters, usually ranging from 4 to 30 angstroms (Cooper and Alley, 1994).

As discussed in Chapter 1, successful regeneration is critical to a wider application of AC adsorption processes. The first significant commercial-scale granular AC regeneration was the burning of spent AC in sugar refineries around 1828. Regeneration in modern sense is aimed to restore the adsorption capacity without much loss of carbon and without much altering the surface of AC. A variety of regeneration techniques have been suggested, evaluated and applied. These methods are based either

on desorption or decomposition. Figure 2-1 shows an overview of available techniques for the regeneration of spent AC adsorbents (Sheintuch and Mataov-meytal, 1999). These regeneration methods have their advantages and disadvantages.

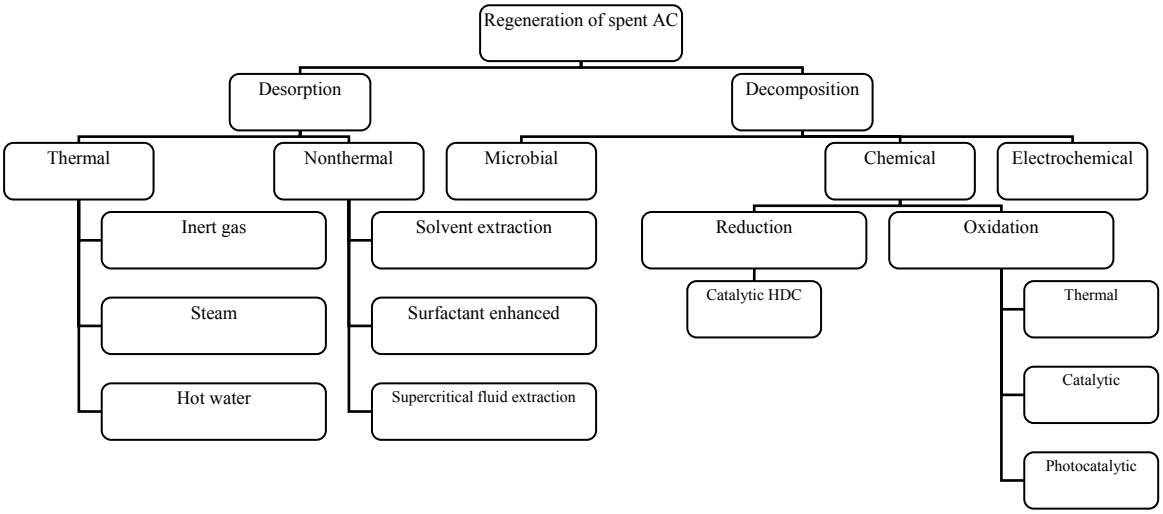

Figure 2-1 Overview of available techniques for AC regeneration (Sheintuch and Mataov-meytal, 1999).

Thermal regeneration is the most commonly used regeneration method which refers to processes of drying, thermal desorption and high temperature reactive treatment (700 – 1000 ^{o}C) in the presence of inert gas or limited quantities of oxidizing gases such as water vapor of flue gas. The thermal regeneration behavior of the AC loaded with various compounds has been studied (Sheintuch and Matatov-Metal, 1999). Spent AC undergoes the following scenario with increasing temperature: drying and loss of highly volatile compounds occurs at temperatures below 200 ^{o}C, vaporization and decomposition of unstable compounds takes place at 200 < T < 500 ^{o}C and pyrolysis of nonvolatile adsorbates to form char occurs at 500 < T < 700 ^{o}C followed by oxidation of the residue at higher temperatures. Exposure to temperatures of 750 – 980 ^{o}C leads to oxidation of

the residual material as well as that of the carbon itself. The pore structure may be altered in the latter steps where small pores (< 2 nm) are lost while large pores are created.

There are some disadvantages of thermal regeneration. Firstly, it is usually not conducted in situ, requiring special regeneration units such as multiple hearth furnaces or rotary kilns (Sheintuch and Mataov-meytal, 1999; Khan, 2003). Secondly, it typically results in a continuous loss of 5 -15 % per cycle in adsorption capacity and in surface area due to the high-temperature (Sheintuch and Mataov-meytal, 1999). The adsorption capacity may even drop to zero after few cycles. Thirdly, the cost of regeneration is high, accounting for nearly 50% of the entire treatment technique expenditures (Khan, 2003). Generally speaking, thermal regeneration is applicable to all. However, it is economically feasible only for large systems that use more than 500,000 tons of granular AC per year (Sheintuch and Mataov-meytal, 1999). Thermal regeneration depends both on thermal desorption and thermal oxidation. The degree of desorption and oxidation depends on the nature of the adsorbent and the adsorbate and the rate of the process (Sheintuch and Matatov-Metal, 1999). Some undestroyed pollutants and harmful byproducts may get into the environment. Therefore, another disadvantage of thermal regeneration is that some adsorbates, especially highly volatile organic compounds, just desorb. Post-treatment devices may be needed.

Several other regeneration methods have been suggested in recent years, such as solvent extraction, supercritical fluid extraction, surfactant enhanced regeneration, and chemical oxidation using various oxidants (chlorine, chlorine dioxide, peroxide, ozone, and potassium permanganate). However, these methods have not proven technically

feasible for continuous operation, nor economically viable (Sheintuch and Mataov-meytal, 1999).

Photocatalytic oxidation is one recently suggested method that can be used to regenerate spent AC adsorbent and destroy organic adsorbates simultaneously (Crittenden et al., 1993; Liu et al., 1996). The advantages of heterogeneous photocatalysis over other regeneration methods include:

1. It can destroy a wide variety of organic compounds (Hoffmann et al., 1995);
2. No post-treatment is needed since the organic pollutants can be mineralized into nontoxic by-products such as H_2O, CO_2, and mineral acids (Hoffmann et al., 1995; Alberici and Jardim 1997) ;
3. The process can be performed at low temperature (Hoffmann et al., 1995; Alberici and Jardim 1997; Pitoniak et al., 2003);
4. It can be promoted by solar radiation, resulting in low energy cost (Crittenden et al., 1997; Malato et al., 2001);
5. On-site regeneration of spent adsorbent and destruction of adsorbed organic material is provided (Crittenden et al., 1993);
6. The loss of adsorbents due to attrition and burn-off which occurs in thermal regeneration is less (Crittenden et al., 1993).

Several works were carried out in applying AC adsorption and photocatalytic regeneration in water treatment. Crittenden and coworkers studied the removal of trichlorethene (TCE) and *p*-dichlorobenzene (DCB) from water by Pt-TiO_2 coated AC (Filtrasorb-400). Based on this study, the photocatalytic regeneration process was found to be limited by reaction rate at the beginning of the regeneration cycle and then by desorption of the adsorbates from the interior of the AC. The photocatalytic regeneration for water treatment was a very long process which makes it unsuitable for this practical application (Crittenden et al., 1996). The diffusibility of molecules in air is faster than that in water. The gas phase application of photocatalytic regeneration may be suitable.

The objective of this chapter was to study the technical efficacy of photocatalytic regeneration in gas phase application. The model pollutant, methanol, was removed from humid air stream by using combined AC adsorption and photocatalytic regeneration. To achieve this objective, TiO_2/AC composite was prepared by a low-cost spray desiccation method. The removal of methanol and the regeneration performance were tested. The effect of humidity on adsorption and photocatalytic oxidation and the effect of purge air on photocatalytic regeneration were further studied.

Experimental Section

Catalyst and Chemicals

The TiO_2 photocatalyst used in this study was Degussa P25 titanium dioxide. Research on the use of Degussa P25 has been reported in numerous articles (Lu et al., 1999; Pozzo et al., 2000; Bhatkhande et al., 2001; Liu et al., 2004; Jeong et al., 2004). AC used in this study was MeadWestvaco BioNuchar 120 (a wood based chemically AC, 8 – 12 mesh). The BioNuchar 120 was selected because it possesses the best methanol adsorption capacity among various carbons tested, according to a previous study (Stokke, 2003). TiO_2/AC composite is prepared by a spray desiccation method. The P25 slurry was sprayed on AC and then dried in a rotary kiln. The methanol/air mixture cylinder (1000 ppm) was purchased from the Praxair Company.

Characterization

The specific surface area and pore size distribution of the carbon and TiO_2/AC samples were obtained by N_2 adsorption/desorption isotherms performed at 77 K (NOVA 1200, Quantachrome). All samples were dried at 110 ^oC for 2 h prior to measurement. The specific surface area was determined by multipoint BET (Brunauer, Emmett, and Teller) method using the adsorption data in the relative pressure (P/P_0) range of 0.05-

0.30. The isotherms were used to determine the pore size distribution using the Barrett, Joyner, and Halenda (BJH) method. The surface morphology of TiO_2/AC composites was characterized by Scanning Electron Microscopy (JSM6330F, JEOL).

The amount of P25 TiO_2 and AC added in this procedure depended on the experimental conditions. The TiO_2 loading on the AC was determined by ash content analysis. Both virgin AC and TiO_2/AC composite were combusted in an oven at 600 ^oC for 4 h. After combustion in the oven at 600 ^oC for two or more hours, the mass of the material did not further change. Based on the condition that the ash content of carbon remains the same for both the AC and TiO_2/AC, the loading of TiO_2 can then be determined by the following equation,

$$W_{TiO2} = \frac{W_{R,T} - W_{ash}}{1 - W_{ash}} \qquad (2\text{-}1)$$

where, W_{ash} (%) is the ash content of AC (i.e. the residual mass of virgin AC after combustion); $W_{R,T}$ (%) is the residual mass of TiO_2/AC after combustion; W_{TiO2} (%) is the TiO_2 loading.

Methanol Removal Evaluation

In order to simulate the emissions from paper mills, a low methanol concentration and high humidity were chosen. The experimental set up is shown in Figure 2-2. One gram of TiO_2/AC was placed on the frit in the reactor which was equipped with an 8 W black light UV lamp (peak wavelength at 365 nm) at the center of the reactor. The distance between the UV lamp and the inner wall of the reactor is 9 mm. The outer diameter of the reactor is 48 mm. The methanol concentration in the influent and effluent of the reactor during the experiment was measured according to the NCASI chilled impinger test method (Method CI/SG/PULP-94.02). The methanol in the air flow was

first collected by drawing it through two midget impingers (Analytical Research Systems, Inc.) in series which were filled with 10 mL of water. The impingers were kept in an ice water bath (around 2 ^{o}C) during sampling to enhance collection efficiency. The sampling time was 1 h. The methanol concentration in the impingers was analyzed by direct injection into a gas chromatograph (Clarus 500, Perkin Elmer) equipped with a flame ionization detector (GC/FID). Cyclohexanol solution (3 mg L^{-1}) was used as an internal standard. The methanol calibration curve is liner (correlation coefficient grater than 0.99) throughout the range of the calibration curve (0.5 – 100 mg L^{-1}).The methanol removal performance of different samples was evaluated by the concentration of methanol in the effluent. Formaldehyde is one of the possible intermediate products of methanol photocatalytic oxidation (Araña et al., 2004). The NCASI chilled impinger method (Method CI/WP-98.01) was used to measure formaldehyde concentration. A 2.0 mL aliquot of the impinger sample was mixed thoroughly with 2.0 mL of acetylacetone reagent and reacted in a water bath at 60 ^{o}C for 10 min. After cooling to room temperature, the absorbance of the solution at 412 nm was measured by a spectrophotometer (DR/4000U, HACH). Formaldehyde concentration was calculated according to a standard calibration curve. The formaldehyde calibration curve is liner (correlation coefficient grater than 0.99) throughout the range of the calibration curve (0.5 – 10 mg L^{-1}).

Due to the high humidity in the atmospheric emission of pulp and paper mills, before testing 1.00 g TiO_2/AC sample was prehumidified until equilibrium was established at a constant stream humidity (RH ≈ 80% at 298 K, water vapor concentration was 19 mgL^{-1}) which was achieved by bubbling the carrier gas (air) through the vessel

with water at the rate of 0.4 $Lmin^{-1}$. Humid methanol laden air was then passed through the fixed bed of TiO_2/AC with or without UV light for 6 h. With UV light irradiation, the temperature in the reactor rose to 328 K due to the heat release from the UV lamp and the relative humidity dropped to 16%. The bed depth was 0.4 cm and the empty bed contact time (EBCT) was about 0.35 s. EBCT is determined by dividing the volume of the carbon bed (L) by the airflow rate (L min^{-1}). Note that the actual contact time is less than the EBCT because the carbon fills much of the bed volume. Air flows through only the void space that is smaller than the entire bed volume. EBCT is used in the study because the actual contact time is difficult to measure. In order to investigate the effect of EBCT, methanol removal performance in 7.00 g TiO_2/AC (prehumidified) column with and without UV irradiation was also tested. The bed depth was 2.8 cm and the EBCT was 2.45 s.

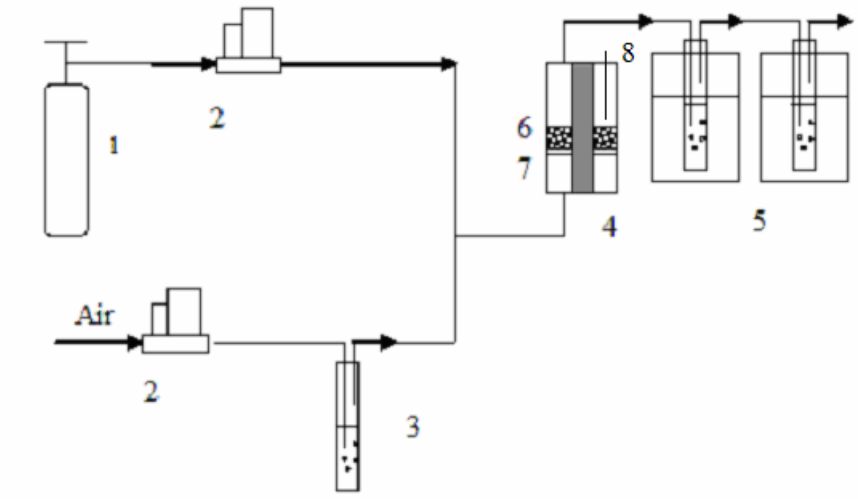

Figure 2-2 Setup of experimental apparatus: 1. Methanol/Air mixture cylinder (1000 ppmv MeOH); 2. Mass flow controller; 3. Water bubble bottle; 4. Photocatalytic reactor (equipped with an 8 W black light UV lamp); 5. Impingers in ice bath; 6. TiO_2/AC; 7. Frit; 8. Thermocouple

In order to evaluate the effect of water on methanol adsorption and photocatalytic oxidation, experiments were also carried out without prehumidification and/or in dry

airstreams. Table 2-1 lists the experimental conditions using 1.00 g TiO_2/AC to evaluate the effect of water on adsorption and photocatalytic oxidation (Set 1-3). In order to reduce the operation cost, adsorption followed by periodic photocatalytic regeneration of TiO_2/AC was tested. Experiments were carried out following the similar procedure used in Sets 1-3. Methanol laden air was passed through the fixed bed of 1.00g TiO_2/AC without UV light (T = 298 K) for 6 h. The flow was then cut off and the UV light was turned on to regenerate the spent carbon for 3 to 9 h (T = 328 K). The adsorption-regeneration cycle was repeated four times. The methanol adsorption capacity of each cycle was determined. The effect of purge air flow rate in regeneration was also investigated.

Table 2-1 The experimental conditions of methanol removal*

Set	Prehumidification	RH	Operation	Regeneration
1	Yes	80%	6 h, with or without UV light	--
2	No	80%	6 h, with or without UV light	--
3	No	0%	6 h, with or without UV light	--
4	Yes	80%	6 h without UV light	9 h between the 1st and the 2nd cycles; 6 h between the 2nd and the 3rd cycles; 3 h between the 3rd and the 4th cycles; all without purge air
5	No	80%	6 h without UV light	3 h, without purge air
6	No	0%	6 h without UV light	3 h, without purge air
7	No	0%	6 h without UV light	3 h, with 0.1 L/min purge air
8	No	0%	6 h without UV light	3 h, with 0.2 L/min purge air

* EBCT = 0.35 s

Table 2-1 also lists the experimental conditions using 1.00 g TiO_2/AC to evaluate the effect of water on regeneration (Set 4-6) and the effect of purge air flow rate on regeneration (Set 6-8).

Results and Discussion

TiO_2/AC Characterization

Figure 2-3 shows the SEM images for the TiO_2/AC composite prepared by the described method. The SEM image of the external surface indicates the P25 TiO_2 particles were coated on the AC surface by the described method. Although the primary particle size of P25 is about 20 nm (Degussa AG, TI 1234), the P25 nanoparticles on the carbon surface were agglomerated. The difference between the SEM images of the external and internal surface of the TiO_2/AC particle indicates that the TiO_2 was mainly coated on the outer surface of the AC particles. The TiO_2 loading was 7.61 ± 0.20 wt % measured by the ash analysis method described earlier. Table 2-2 lists the specific surface area and pore size distribution of AC before and after TiO_2 coating. The BET surface area measurement of one F400 AC (coal based thermally activated, Calgon) sample was repeated three times. The results were 733, 742, and 745 m^2/g. The reproducibility was 0.84%. Because of the inhomogeneity of AC, the reproducibility of different AC samples (same type of AC) is even higher. The BET surface area measurement of F400 AC (different samples) was repeated five times. The results were 618, 653, 709, 740, and 745 m^2/g. The reproducibility was 8.03%. Therefore, the TiO_2 coating didn't significantly change the BET surface area of the AC which indicated that the TiO_2 particles just coated on the external surface of AC.

Table 2-2 BET surface area and pore size distribution of AC and TiO_2/AC

	BET (m^2g^{-1})	Total Pore Volume (ccg^{-1})	Micropores (ccg^{-1})	Mesopores (ccg^{-1})
AC	1472	1.45	0.46	0.84
TiO_2/AC	1380	1.38	0.54	0.79

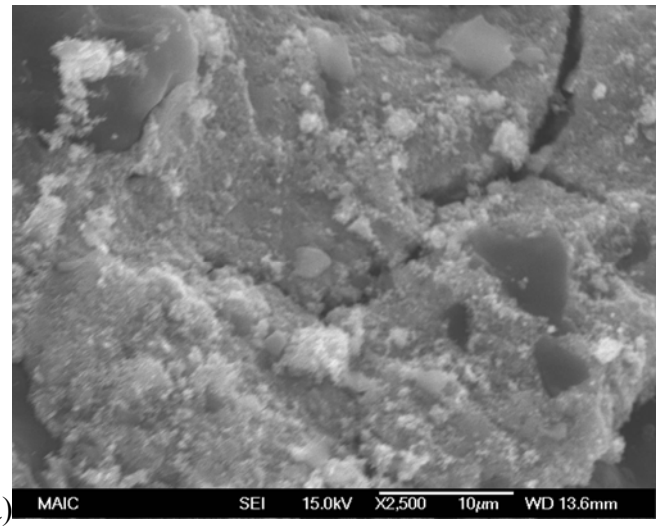

(a)

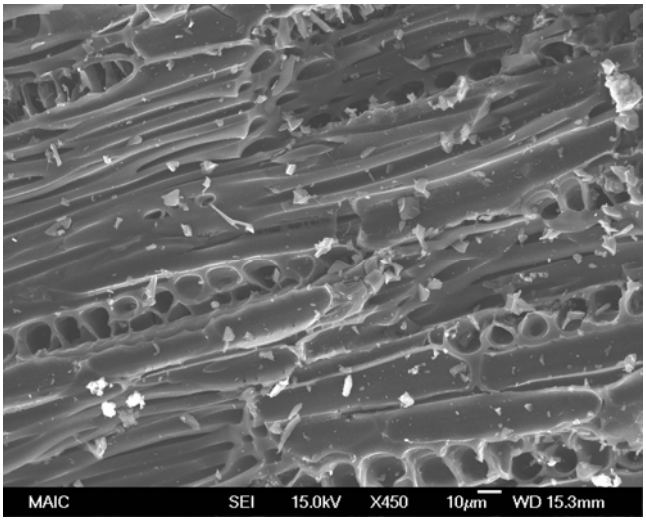

(b)

Figure 2-3 SEM images for the TiO_2/AC composite: (a) external surface; (b) internal surface.

Methanol Removal by Adsorption and Adsorption/Photocatalytic Oxidation

The efficiency of the virgin AC and TiO_2/AC composites for methanol removal was evaluated in the presence and absence of UV light. The relative effluent methanol

concentration profiles for the virgin AC and TiO_2/AC are shown in Figure 2-4. It is apparent from Figure 2-4 that the effluent methanol concentration increased quickly when treated by the virgin AC with and without UV light. The effluent concentration was higher when treated with UV light probably due to the heat released by UC lamp. When treated by TiO_2/AC without UV light irradiation, a similar adsorption profile was observed, and the methanol adsorption capacities for the virgin AC and TiO_2/AC composite were similar. However, when methanol was treated by the TiO_2/AC with UV light irradiation, the methanol concentration didn't reach saturation for the duration of the experiment. The effluent methanol concentration increased during the first 2 h and then remained almost constant (~35% removal). Figure 2-5 displays the methanol effluent concentration when using 7.00 g TiO_2/AC composite. As shown, increasing the EBCT increased the methanol removal. Under UV irradiation, the methanol removal efficiency remained stable around 90% for 12 h. These two sets of experiments show that photocatalytic oxidation can be used to destroy methanol adsorbates simultaneously and to extend the AC's usage life.

Effect of Water

In order to investigate the effect of water on methanol adsorption and photocatalytic oxidation, several experiments were carried out as described in Table 2-1 (Sets 1-3). Figure 2-6 shows the relative effluent methanol concentration.

It is well known that the adsorption of organic vapors on AC can be disturbed by the presence of water vapor because of the molecular interactions that account for the various nonidealities exhibited during the coadsorption of the mixture. Typically, the adsorption of organic compounds exhibit a type I isotherm (Taqvi et al., 1999; Finqueneisel et al., 2005). As a result, much of the pore volume is filled at low relative

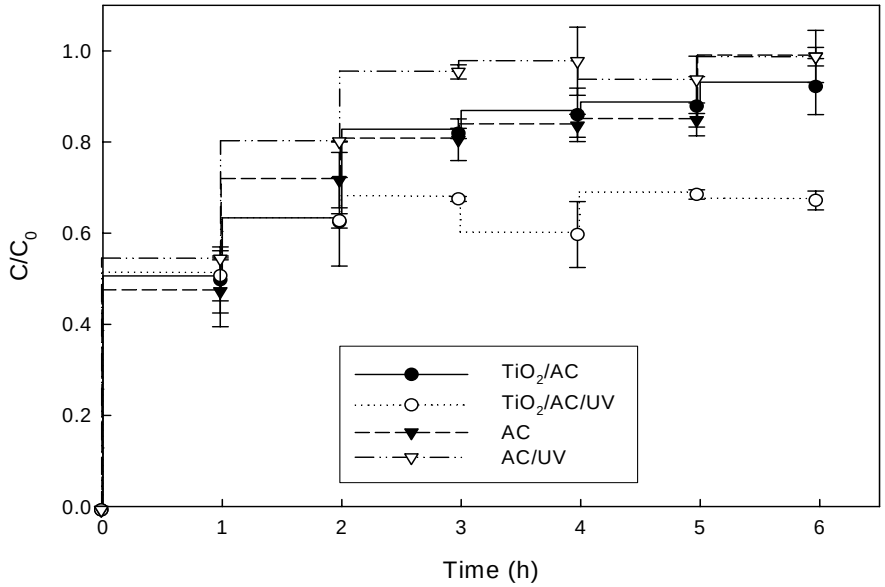

Figure 2-4 The relative effluent methanol concentration profiles for the virgin AC and TiO_2/AC (C_0= 31.0 ppm, EBCT=0.35 s).

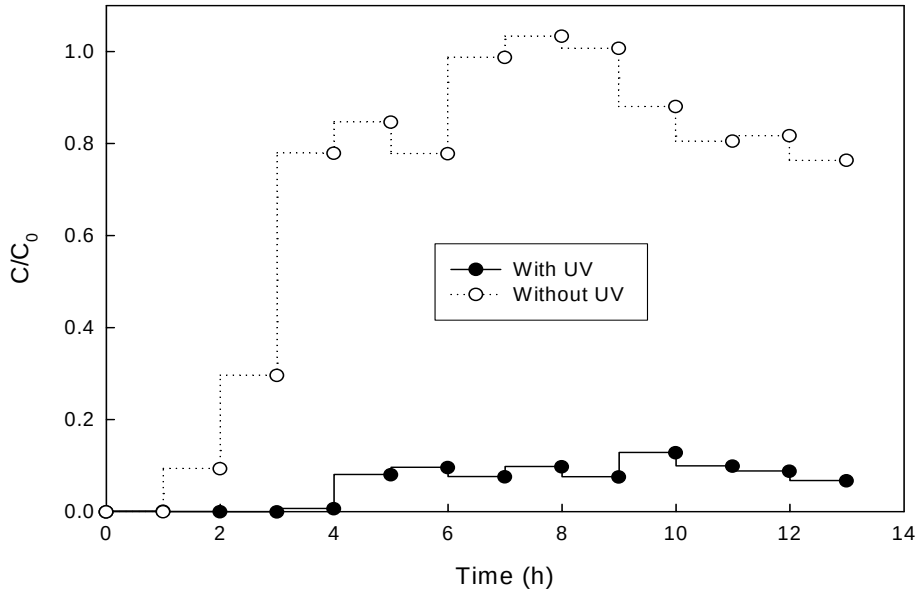

Figure 2-5 The relative methanol effluent concentration of 7 g TiO_2/AC composite (C_0=36.4 ppm, EBCT = 2.45 s)

pressures. Water dose not interact strongly with carbonaceous solids and exhibits a type V (S-shaped) isotherm on AC (Taqvi et al., 1999; Finqueneisel et al., 2005). At higher

relative humidity values (>40 to 50%) the moisture adsorption increases sharply due to capillary condensation. The adsorbed water fills the small pores in the adsorbent and can interfere with the adsorption capacity of organic compounds (Noll, 1999). Methanol is a polar molecule and is miscible in water. Taqvi et al. (1999) reported water promoted the adsorption of methanol on BPL AC by the ability of alcohol to form H bond with water. Friqueneisel et al. (2005) developed a model of adsorption isotherms of methanol/water vapor mixture on microporous AC (hydrophobic surface). This model predicted that the amount of methanol adsorbed at RH = 42% is equal to the amount of methanol adsorbed in dry conditions. Below this value the amount of methanol adsorbed is lower than in dry conditions and above this value the amount is higher than in dry conditions. Gubkina et al. (2003) studied the adsorption of gas phase methanol on a humidified AC (T = 293 K, RH = 75%). Within their studied concentration range (methanol < 0.2 mg L^{-1}), the adsorption for methanol on humidified AC in the presence of water vapor (T = 293 K, RH = 75%) has a weakly concave shape and can be considered to be linear.

Our results of methanol removal without UV light (Figure 2-6 a) show that high humidity greatly hindered the methanol adsorption on TiO_2/AC. The methanol adsorption capacity of Set 1 and Set 2 was much lower than that of Set 3. This result is different form the results of Taqvi et al. (1999) and Friqueneisel et al. (2005). The difference is due to the different conditions tested. Their results were based on equilibrium adsorption and our results were based on fixed-bed breakthrough experiments and the bed depth was short. For Set 1, TiO_2/AC was humidified. Compared with Set 2, the methanol adsorption was higher in the beginning due to the formation of hydrogen bond with water molecules.

However, the difference diminished later because the adsorbed water filled the pores resulting in less space available for adsorption.

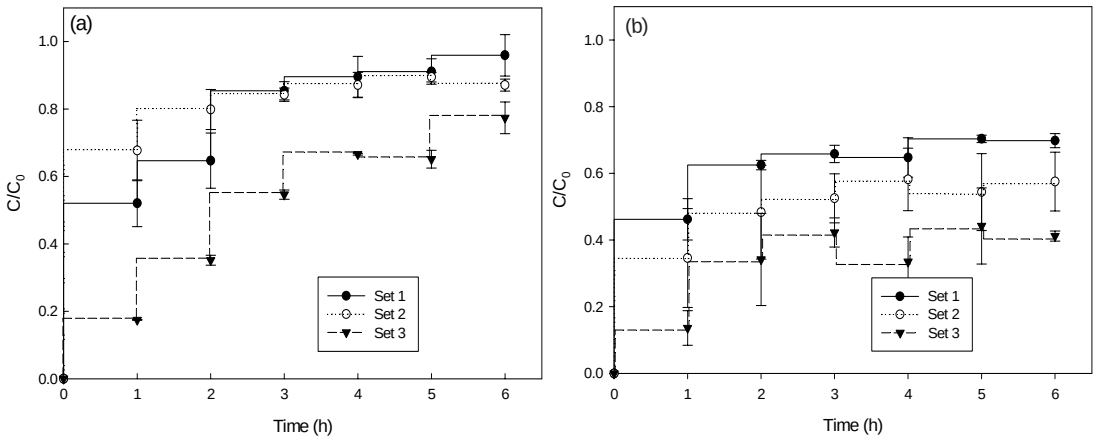

Figure 2-6 The relative effluent methanol concentration for Sets 1, 2 and 3: (a) without UV light; (b) with UV light. (C_0=31.0 ppm)

With UV light irradiation, the temperature rose to 328 K and the RH decreased to 16%. When adsorption is an exothermic process, the adsorption of both methanol and water decreased with the increase of temperature. Therefore, the photocatalytic oxidation is the main mechanism of methanol removal under UV light irradiation. The results of methanol removal with UV light (Figure 2-6 b) show that methanol oxidation on TiO_2/AC was improved in dry condition. This result is in concord with the results of Kim and Hong (2002) that the photocatalytic degradation rate of methanol was relatively high in lower water vapor concentration and that high humidity (RH > 10.6%, T = 318 K) hindered the photocatalytic degradation of methanol. The influence of water vapor on the photocatalytic oxidation has been reported by many researchers. Although water plays an important role in the formation of the hydroxyl radicals, adsorbed water is an effective electron-hole recombination center leading to less photocatalytic activity (Linsebigler et

al., 1995; Chang et al., 2005). Hence, high concentration of water vapor reduces the adsorption of organic vapor and leads to the inhibition of methanol oxidation.

Regeneration Performance

The advantages of the integration of adsorption and photocatalytic regeneration are that the photocatalytic oxidation on TiO_2/AC can be accelerated by the high concentration of pollutants eluted from the adsorbent and can reduce the UV irradiation time, thus improving the economy of the process. Moreover, the regeneration process can be operated in-situ at ambient conditions. Figure 2-7 shows the adsorption breakthrough curves of methanol from fresh and regenerated beds of TiO_2/AC of Set 4. Figure 2-7 shows the adsorption capacity of each cycle of Sets 4, 5 and 6.

For Set 4, Figures 2-7 and 2-8 show that around 60% of the virgin capacity of the TiO_2/AC was regenerated and increasing the regeneration time did not increase the regeneration capacity. Therefore, 3 h regeneration was used in Set 5 and Set 6. For Set 5, the virgin capacity was slightly higher than that of Set 4. This result is consistent with the result of Figure 2-6a. The regeneration capacity of cycles 2, 3 and 4 of Set 5 was around 80%, 74% and 60% of the virgin capacity, respectively. In the first 3 cycles of adsorption, the TiO_2/AC was not saturated with water vapor. That resulted in a higher capacity of Set 5 compared to Set 4. After 3 cycles of adsorption, the TiO_2/AC was almost saturated with water vapor. Therefore the regeneration capacity of the 4^{th} cycle of Set 5 was similar to that of Set 4. For Set 6, Figure 2-8 shows that the virgin capacity was 1.8 times of the virgin capacity of Set 4. This result was consistent with the result of Figure 2-6a. However, the regeneration capacity of Set 6 was quite similar to that of Set 4. That indicated just the outer layer of the TiO_2/AC was regenerated where the UV light can reach and where the TiO_2 coating is. This is consistent with the finding reported by

Crittenden et al. (1997) that the photocatalytic regeneration process was limited by the desorption of the adsorbate from the interior of the carbon.

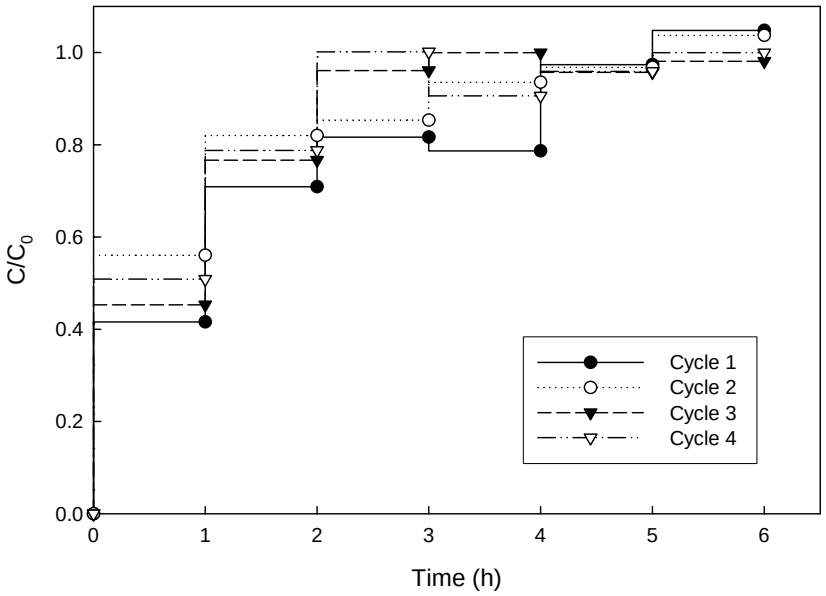

Figure 2-7 The adsorption breakthrough curves of methanol from fresh and regenerated beds of TiO_2/AC of Set 4 (C_0 =31.0 ppm).

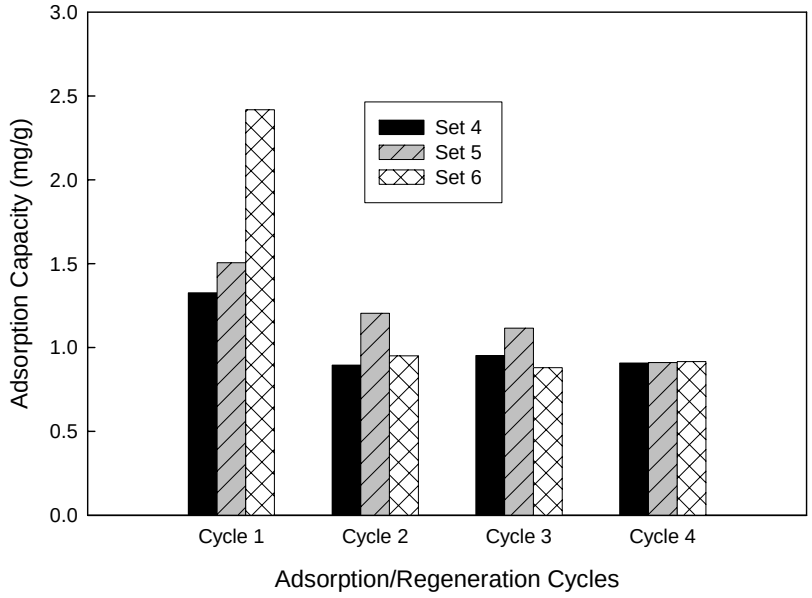

Figure 2-8 The adsorption capacity of each cycle of Set 4(C_0 =31.0 ppm), 5 (C_0= 34.3ppm) and 6 (C_0 =27.6 ppm)

A possible way to increase the regeneration capacity is to increase the desorption rate through heating or purging. Therefore, purge air was used to increase the desorption rate and the effect of purge air flow was investigated. During regeneration, the methanol and formaldehyde in reactor effluents were collected and measured. Figure 2-9 shows the amount of methanol adsorbed, the amount of methanol desorbed in purge air and the amount of formaldehyde formed in regeneration in each cycle of Sets 7 and 8.

When using 0.2 L min^{-1} purge air (Set 8), around 77% of the original capacity was regenerated after 3 h regeneration. Around 52% regeneration capacity resulted from direct desorption. When using 0.1 L min^{-1} purge air (Set 7), around 80% of the original capacity was regenerated after 3 h regeneration. Around 24% regeneration capacity resulted from direct desorption. Without purge air (Set 6), only 40% of the original capacity was regenerated after 3 h UV irradiation.

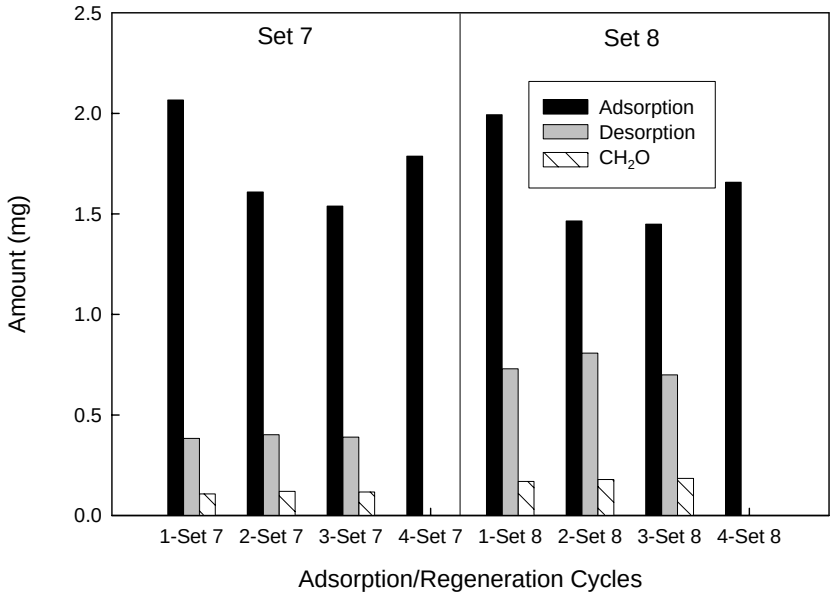

Figure 2-9 The methanol adsorption amount in adsorption, methanol desorption and formaldehyde formation amount in regeneration of each cycle of Sets 7 and 8 (C_0 =23.7 ppm)

Photocatalytic regeneration of AC is ascribed to both desorption from AC and photocatalytic degradation on TiO_2. Therefore, both the desorption rate and degradation rate affect the regeneration efficiency. Without purge air, desorption rate from AC was so low that the methanol adsorbed on the carbon could not be effectively transferred to the TiO_2 photocatalyst. Hence, the photocatalytic regeneration process was limited by the desorption rate. With 0.1 L min^{-1} purge air, the regeneration efficiency was greatly increased. If the desorption rate was higher than the degradation rate, part of the methanol directly desorbed without degradation as demonstrated by the comparison of Sets 7 and 8. With 0.2 L min^{-1} purge air, the desorption rate was greatly enhanced although the regeneration efficiency decreased because of the decreased degradation rate resulting from the reduction in contact time. Furthermore the formaldehyde formation of Set 7 was lower than that of Set 8. This further indicates that the contact time was not enough for complete photocatalytic oxidation. Without purge air (Set 6), there should be no incomplete degradation product formed because the contact time was much longer. Based on the above mentioned results, the photocatalytic degradation should reach maximum when the rate of degradation and the rate of desorption match with each other.

Conclusions

Photocatalytic oxidation can be used to regenerate spent adsorbent (Bio-Nuchar AC) and destroy methanol simultaneously. The photocatalyst loaded onto the AC has no significant impact on the adsorption capacity of the AC. Increasing the EBCT from 0.35 s to 2.45 s can significantly increase the efficiency of the simultaneous adsorption and photocatalytic oxidation. High humidity can reduce the effectiveness of methanol adsorption and simultaneous adsorption and photocatalytic oxidation on TiO_2/AC. The regeneration process is limited by desorption of adsorbate from the interior surface of the

carbon. Increasing desorption rate can significantly increase the regeneration capacity. However, when the rate of desorption is greater than the rate of photocatalytic oxidation, part of the methanol directly desorbs without degradation.

CHAPTER 3
PREPARATION OF TiO_2/AC COMPOSITE PHOTOCATLYST BY DRY IMPREGNATION

Introduction

Recently, several works were carried out on the preparation and application of TiO_2/AC composite photocatalyst. Few works prepared TiO_2/AC during the activation of carbon, such as carbonization of a mixture of coal and TiO_2 or TiO_2 precursor (Aikyo et al., 1996; Przepiorski et al., 2001). Most works used commercially available AC as the raw material. The deposition of TiO_2 nanophotocatalyst on commercial AC can be categorized into chemical and physical methods. The chemical methods mainly rely on hydrolysis of titanium alkoxides such as chemical vapor deposition (El-Sheikh et al., 2004), impregnation (Harada et al., 1999) and sol-gel method (Capio et al., 2005). The physical methods use commercially available photocatalyst. Examples include spray desiccation (Lu et al., 1999), mechano-fusion (Khan, 2003), dip-coating (Jeong et al., 2004), and spray desiccation technique (used in Chapter 2). However, the best methods and experimental conditions of carrying out the process are not yet clear because of the high porosity and non-homogeneous nature of AC. The inhomogeneity makes it difficult to produce homogeneous distribution of TiO_2 on the surface of AC (El-Sheikh et al., 2004). Furthermore, UV light cannot penetrate into pores rendering TiO_2 nanoparticles deposited inside the pores useless. Therefore, TiO_2 nanoparticles deposited on the outer surface of activated carbon is desired.

Impregnation is a commonly used method in supported catalyst preparation. Impregnated catalysts are usually obtained from preformed supports by impregnation with the active phase. The impregnation method involves three steps: (1) contacting the support with the impregnating solution for a certain period of time, (2) drying the support to remove the imbibed liquid and (3) activating the catalyst by calcination, reduction or other appropriate treatment. Two methods of contacting, wet impregnation and dry impregnation, may be distinguished, depending on the total amount of solution (Perego and Villa, 1997). The principle of dry impregnation is that the volume of the precursor solution used in the impregnation is equal to the pore volume of the support, which results in a better distribution of the solute on the support surface (Huang et al., 2002).

The advantages of impregnation method include:

- The process can be performed continuously in industry.
- It produces uniform coating with good reproducibility and adhesion;
- It controls crystal structure and surface morphology of the TiO_2 by controlling the process parameters.

The spray desiccation coating method used in this Chapter 2 can effectively coat commercial TiO_2 on AC. However, the nanoparticles of TiO_2 were agglomerated on the carbon surface which reduced the photocatalytic efficiency. Besides, this coating method is a physical method. The TiO_2 particles were coated on the carbon surface by weak physical force. In order to improve the photocatalytic efficiency and the adherence between TiO_2 photocatalyst and carbon support, dry impregnation method was used to prepare TiO_2/AC composite photocatalyst in this chapter. Although impregnation method has been adopted in TiO_2/AC preparation before, very few studies have been carried out to prepare TiO_2/AC composite using titanium tetra-isopropoxide precursor and

information about the preparation details is very limited. This chapter focused on the understanding of the effects of various preparation parameters (hydrolysis temperature, hydrolysis time, water vapor concentration, precursor concentration, and moisture content of AC) of the synthetic method. The prepared TiO_2/AC composite photocatalyst was also evaluated by removing low concentration methanol from humid air stream.

Experimental Section

Materials

All chemicals were reagent grade or better: titanium tetra-isopropoxide (TTIP) ($Ti(OC_3H_7)_4$, 98+%, Fisher); 2-proponal (99.9%, Fisher); methanol/air mixture (1000 ppmv, Praxair); AC (Bio-Nuchar120, wood based chemically activated carbon, 8-16 mesh, pore volume of 1.45 cc/g, MeadWestvaco), commercial TiO_2 photocatalyst (Degussa P25).

Material Preparation

The TiO_2/AC composites were prepared by dry impregnation using a TTIP solution (with 80 vol % of 2-propanol) followed by hydrolysis and calcination. The TTIP solution was stored in sealed container. No hydrolysis in the solution was observed. Before coating, the AC was heated at 105 ^oC for 4 h to remove moisture. The carbon (3.5 g) was then mixed with 5 mL of TTIP solution and immediately placed in a hydrolysis reactor, as shown in Figure 3-1. The diameter of the reactor is 1 inch, and the pore size of the support frit to better distribute the air flow is 25-50 μm. Air saturated with water from a humidifier was passed through the reactor at 0.75 L/min for 2 or 24 h. The empty bed contact time was 0.8 s. The temperature of the humidifier was maintained at 25 or 90 ^oC by a hot plate with a temperature controller to determine the effect of moisture content.

The temperature of the reactor was controlled at 25, 90, or 175 ^{o}C, depending upon the desired synthesis strategy, by heating tape wrapped around the reactor. The various hydrolysis conditions are summarized in Table 3-1. After hydrolysis, the samples were dried at 105 ^{o}C for 4 h to evaporate the adsorbed 2-propanol and then calcined at 300 ^{o}C for 2 h in air. This calcination condition was chosen according to Colón et al. (2002) who reported that TiO_2/AC samples (prepared by means of sol-gel precipitation from TTIP) calcined under this condition showed higher photon efficiency. Other different calcination conditions were also investigated for their effects on product properties. Considering that carbon will partly gasify during calcination in air, calcination in N_2 was also performed. Table 3-2 lists the calcination conditions. Samples 6-8 listed in Table 3-2 were prepared by 20 vol % TTIP solution and hydrolyzed in an open vessel under humid air (RH = 47 %) for 24 h. BioNuchar AC coated with 9 wt % P25 photocatalyst by spray desiccation method (used in Chapter 2) was used as the baseline for photocatalytic activity evaluation.

Table 3-1 Effect of hydrolysis conditions*

Sample No.	Water bath Temp. (^{o}C)	Hydrolysis Temp. (^{o}C)	Hydrolysis Time (hour)	Specific Surface Area (m^2/g)	TiO_2 Amount (%wt)
1	25	25	2	1113	6.38
2	25	25	24	1150	5.53
3	25	90	2	1140	5.09
4	25	175	2	1018	2.38
5	90	90	2	1270	8.33

* TTIP concentration was 20 vol % in 2-propanol; calcination conditions were the same as sample 7.

The effect of TTIP concentration on the prepared TiO_2/AC was also tested. The TTIP concentration varied from 20 vol % to 5 vol % in 2-propanol. Table 3-3 listed the preparation conditions. Carbon moisture is another important factor that affects the

properties of the prepared TiO_2/AC. Sample 11 was prepared under the same conditions as sample 2 except that the carbon was not dried before preparation.

Table 3-2 Effect of calcination conditions

Sample	Specific Surface Area (m^2/g)	Temp. (^oC)	Atmosphere	Time (h)	Total Pore Volume (cc/g)	Micropores (<20Å) (cc/g)	Mesopores (200-500Å) (cc/g)
AC	1472	-	-	-	1.45	0.46	0.84
AC*	1338	300	air	2.0	NA	NA	NA
6	1265	300	air	0.5	1.35	0.47	0.84
7	1238	300	air	2.0	1.32	0.46	0.78
8**	1479	300	N_2	2.0	NA	NA	NA

* BioNuchar AC calcined at 300 ^{o}C in air

* * Pore volume distribution wasn't measured because the anatase phase was not present

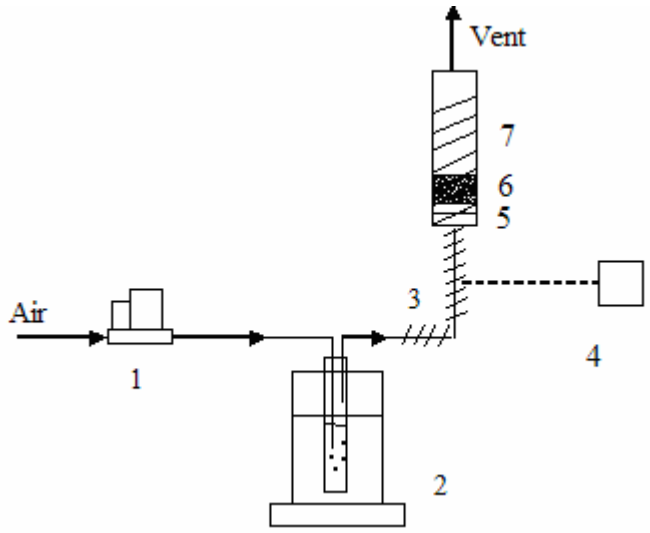

Figure 3-1 Schematic of the hydrolysis reactor: 1. mass flow controller; 2. water bubble bottle with water bath and hot plate (with temperature controller); 3. heating tape; 4. temperature controller; 5. porous frit; 6. carbon loaded with TTIP solution; 7.hydrolysis reactor

Table 3-3 TTIP concentration and carbon moisture*

Sample	Carbon	TTIP Conc. (vol %)	TiO_2 Amount (wt %)
9	Dry	10	4.27
10	Dry	5	2.01 ± 0.17
11	With moisture	20	5.59 ± 0.33

*Other conditions were the same as sample 2.

Characterization

The samples were analyzed by X-ray diffraction (XRD 3720, Philips) for identification of crystalline species in the continuous-scan mode (scanning speed: 0.005^o/sec, scanning range: 20^o to 50^o). The major anatase (101) peak at $2\theta = 25.4^o$ was analyzed. The specific surface area and pore size distribution of the carbon and TiO_2/AC samples were obtained by N_2 adsorption/desorption isotherms performed at 77 K (NOVA 1200, Quantachrome). All samples were dried at 105 ^{o}C for 2 h prior to measurement. The specific surface area was determined by multipoint BET (Brunauer, Emmett and Teller) using the adsorption data in the relative pressure (P/P_0) range of 0.05-0.30. As discussed in Chapter 2, the inhomogeneity of AC resulted in the high deviation of the measured BET surface area. The isotherms were used to determine the pore size distribution using the Barrett, Joyner, and Halenda (BJH) method with cylindrical pore size. The surface morphology of TiO_2/AC composites was characterized by Scanning Electron Microscopy (JSM6330F, JEOL).

The TiO_2 loading on the TiO_2/AC composites were determined using thermogravimetric analysis (TGA, STA 449, NETZSCH). Approximately 20 mg of material was heated up to 1200 ^{o}C at 10 ^{o}C/min under 50 mL min^{-1} air flow. By comparing the resulting ash content of the AC with that of each TiO_2/AC composite, the TiO_2 loading in each composite was calculated according to Equation 2-1 in Chapter 2.

Photocatalytic Activity Evaluation

The same experimental set up used in Chapter 2 (shown in Figure 2-2) was used to evaluate the photocatalytic activity of the composite material thus prepared. One gram of TiO_2/AC was used each time. The TiO_2/AC sample was prehumidified until saturated by passing humid air through the reactor at the rate of 0.4 L/min for 16 h. Methanol laden air

(RH = 80%) was then passed through the fixed bed of TiO_2/AC with and without UV light for 6 h. The empty bed contact time was about 0.35s. The methanol concentration in the influent and effluent of the reactor during the experiment was measured by the same method in Chapter 2. The photocatalytic activity of different samples was evaluated by comparing the concentration of methanol in the effluent. Each test was repeated at least two times.

Results and Discussion

Effect of Calcination Conditions

In order to optimize the formation of anatase, samples prepared by hydrolysis at ambient (25 ^{o}C, RH = 47%) for 24 h and dried at 105 ^{o}C for 4 h were calcined under different conditions (Table 3-2). Figure 3-2 shows the XRD patterns of these samples. By comparing the XRD patterns of samples 6 and 7, it can be seen that the anatase phase was formed during the heat treatment, and the degree of TiO_2 crystallinity increased with longer treatment time. The comparison of the XRD patterns of samples 7 and 8 shows that the anatase phase did not form to the same extent when calcined in N_2 at the same temperature.

The specific surface areas for the samples prepared utilizing different calcination conditions are also listed in Table 3-2. When calcined in air, carbon was partially oxidized and resulted in the decrease of surface area. The specific surface area of BioNuchar AC after calcination (Table 3-2) was 1338 m^2/g, and the weight loss was 4.3 wt %. The surface area of sample 8 did not change a lot from the virgin carbon because the porous structure of the carbon didn't incur serious damage during calcination in N_2. Compared with that of the un-coated Bionuchar, the volume of micropores and mesopores of samples 6 and 7 didn't change significantly. This showed that TiO_2

particles mainly deposited on the outer surface and only slightly in the macropores. This is further confirmed by SEM analyses to be discussed later.

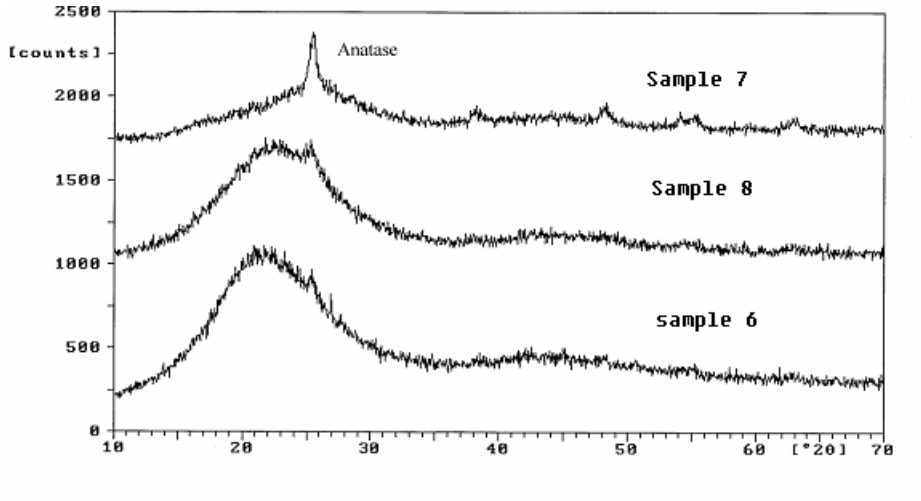

Figure 3-2 XRD patterns of samples calcined under different conditions

In this study, hydrolysis reaction immediately started after mixing the precursor solution with the carbon. The precursor solution might not have sufficient time to penetrate the pores of the carbon. Therefore, TiO_2 just formed on the outer layer of the carbon particle. Since UV light can not penetrate into the carbon, the formation of TiO_2 formation on the outer layer of carbon particles is desired.

In summary, the anatase phase was formed during calcination at 300 ^oC for 2 h in air (sample 7) with minimal carbon loss. This calcination condition was used in the subsequent studies.

Effect of Hydrolysis Conditions

Five hydrolysis conditions were tested (Table 3-1) in order to investigate how these changes effected anatase formation. The specific surface areas for those samples after calcination and the TiO_2 loading derived from TGA measurement described above are also listed in Table 3-1. Figure 3-3 shows the XRD patterns of samples prepared under different hydrolysis conditions. Before calcination, there was no anatase peak on the

XRD pattern; i.e. the as-prepared TiO_2 without calcination was amorphous. Regarding the morphology, Figure 3-4 shows the SEM images of their outer surface.

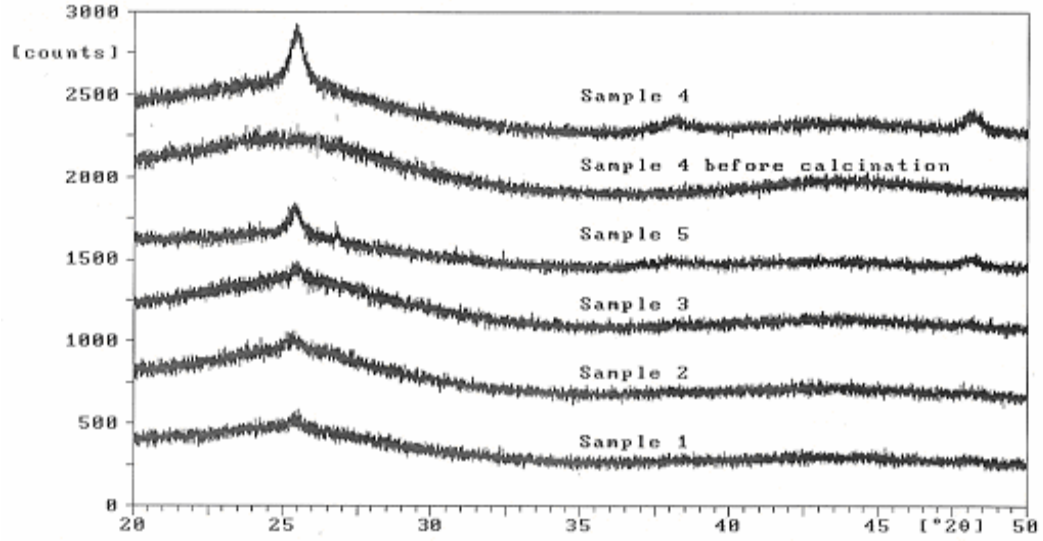

Figure 3-3 XRD patterns of samples prepared under different hydrolysis conditions

Two simultaneous reactions – hydrolysis and polycondensation – take place when TTIP reacts with water. The overall reaction of TTIP occurs as (Seto et al., 1995):

$$TTIP + 2H_2O \rightarrow TiO_2 + 4C_3H_7OH \qquad (3\text{-}1)$$

The vapor phase hydrolysis rate constant k is given by Seto *et al.* (1995):

$$k = 3.0 \times 10^{15} \exp(-8.43 KJ \cdot mol^{-1}/RT)$$

Although the hydrolysis of TTIP in vapor phase is very fast, the hydrolysis of TTIP adsorbed on the carbon is much slower due to mass transfer limitation. There are two possible routes for the adsorbed TTIP to be hydrolyzed: 1) the TTIP desorbs first and then hydrolyzes in vapor phase; 2) the water vapor directly hydrolyzes the adsorbed TTIP.

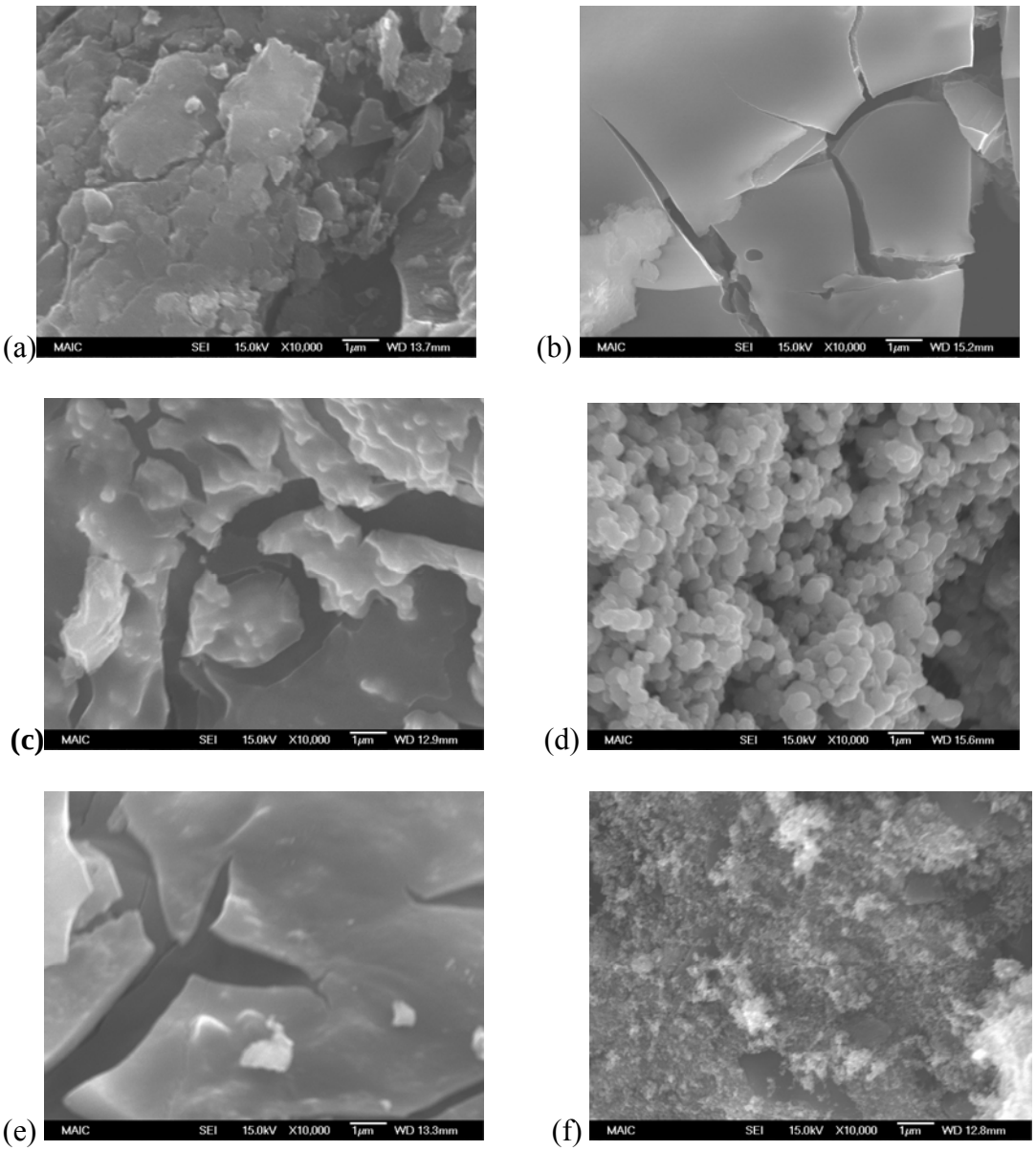

Figure 3-4 SEM images of samples prepared under different hydrolysis conditions (Magnification: 10,000): (a) sample 1; (b) sample 2; (c) sample 3; (d) sample 4; (e) sample 5; (f) 9%P25/AC.

Hydrolysis is the key step for TiO_2 formation in this system. Hydrolysis temperature, hydrolysis time and reactant concentration all effect the hydrolysis reaction. Kinetically, the higher the temperature, the faster the reaction. According to Kim et al. (2000), when the hydrolysis reaction is incomplete, a large amount of unhydrolyzed alkyls remain on the powder. The presence of these alkyls prevents crystallization, thus

keeping TiO_2 in the amorphous phase (Kim et al., 2000). Therefore, the higher the degree of hydrolysis reaction is, the higher the degree of TiO_2 crystallinity. Comparing the XRD patterns for samples 1, 3, and 4, it is clearly demonstrated that the formation of the anatase phase was favored at high hydrolysis temperature. The result concurs with the notion that the hydrolysis reaction is faster at higher hydrolysis temperatures and it agrees with the trend explained by Kim *et al*. (2000). At the same hydrolysis temperature and reactants concentration, increasing the reaction time didn't significantly increase the degree of TiO_2 crystallinity as demonstrated by the similar XRD patterns for samples 1 and 2. In addition to temperature, a higher reactant concentration also results in a faster reaction. Therefore, when the water concentration was higher (sample 5 vs. sample 3), the reaction rate and the major anatase (101) peak at $2\theta = 25.4^{o}$ was higher.

Moreover, the hydrolysis conditions affect the TiO_2 loading and the morphology of TiO_2. Table 3-1 shows that the TiO_2 loading decreased with the increase in hydrolysis temperature due to the increase of desorption of TTIP (boiling point: 220 ^{o}C). The TiO_2 loadings for sample 1, sample 3, and sample 4 were 6.38%, 5.09%, and 2.38% respectively. Although the vapor pressure of TiO_2 is extremely low, TiO_2 molecules formed by hydrolysis need to diffuse to carbon surface and then nucleate. Part of the TiO_2 molecules may be transported by the purge air. Under the same hydrolysis conditions, the TiO_2 loadings for sample 1 and sample 2 were 6.38% and 5.53% respectively. The TiO_2 loading decreased with the increase of hydrolysis time because the loss of TTIP and/or TiO_2 mainly caused by the purge air. The unhydrolyzed TTIP left on the carbon can be hydrolyzed and/or thermally decomposed in the subsequent processes. The TiO_2 thus formed has higher probability to deposit on the carbon surface because of no purge air.

Desorption of TTIP should work the same way under the same hydrolysis temperature for sample 3 and sample 5. The TiO_2 loading of sample 5 (8.33%), however, is higher than that of sample 3 (5.09%). The comparison of these two conditions evidences that the TiO_2 loading positively correlates with the rate of hydrolysis when desorption of TTIP works the same. It should be noted that the theoretical TiO_2 loading (assuming all the TTIP on the carbon is converted to TiO_2) is 8.24%. That indicates all TTIP can be converted to TiO_2 under proper hydrolysis conditions.

Figure 3-4 shows the SEM images of different samples. TiO_2 formed a rough particulate coating layer on the sample 4, and dense coating layers on the other samples. The results presented in the previous paragraph demonstrated that TTIP desorption into the gas phase followed by vapor phase hydrolysis was the main route for the formation of hydrolyzed titanium compounds. The subsequent nucleation of hydrolyzed titanium compounds follows a LaMer type nucleation process (Figure 3-5) (Giesche, 1998). Heterogeneous nucleation doesn't start until the hydrolyzed titanium compounds concentration reaches above the saturation vapor pressure. If the critical nucleation concentration is never exceeded, the system is forced to follow a heterogeneous nucleation and growth mechanism (Curve I in Figure 3-5). Dense coating layers with a uniform thickness are formed (Giesche, 1998). When the critical nucleation concentration is exceeded, homogeneous nucleation is preferred. A lot of nuclei are formed which then relieve the supersaturation (Curve II). Part of those nuclei may also deposit on the carbon surface due to heterocoagulation. When the concentration of hydrolyzed titanium compounds falls below the critical nucleation concentration, heterogeneous nucleation is preferred again and results in the subsequent uniform growth on the existing nuclei

(Giesche, 1998). Therefore rough particulate coating layers formed on sample 4 because the TTIP desorption rate was high enough for the formed hydrolyzed titanium compounds concentration to exceed critical nucleation concentration. Dense coating layers formed on other samples because the critical nucleation concentration wasn't exceeded. The SEM image for the sample prepared by spray desiccation (9% P25/AC) was also shown in Figure 3-4. Although the primary particle size of P25 is about 20 nm, coating thus prepared consisted of agglomerated particles on the carbon surface. The distribution of P25 on TiO_2/AC prepared by spray desiccation was not well dispersed compared to the TiO_2 on the samples prepared by the described method.

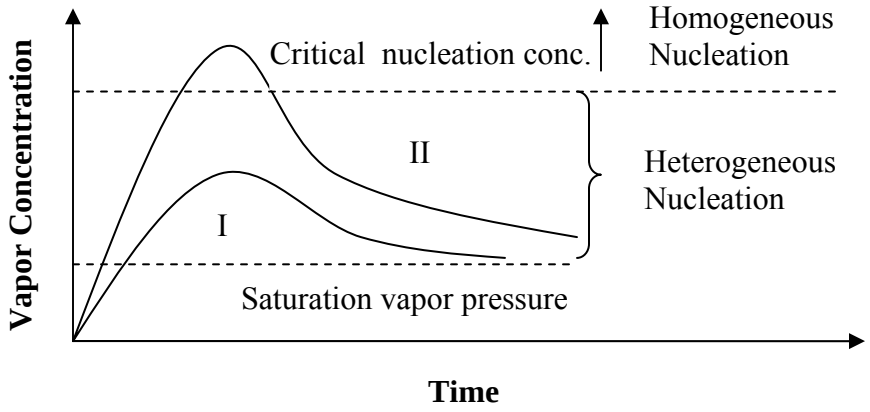

Figure 3-5 The LaMer diagram related to nucleation and growth mechanism

Figure 3-6 shows the SEM image of sample 2's inner surface. Compared with the SEM image of sample 2's outer surface (Figure 3-4), it indicates TiO_2 was mostly coated on the outer layer of the AC. This is consistent with the pore size distribution measurements.

In summary, the hydrolysis reaction rate positively correlated with the hydrolysis temperature and the reactant concentration. Low hydrolysis temperature and shorter hydrolysis time can reduce the vaporization loss of TTIP. Regarding the TiO_2

morphology, high hydrolysis temperature results in particulate coating layer with higher surface area than dense coating layer. Although sample 4 satisfied the requisites for higher photocatalytic activity, large surface area and high crystallinity (Kominami et al., 1997), the hydrolysis conditions of sample 2 were used in the following sections. This is because: 1) carbon is flammable and heating in air poses a hazard of self-ignition; 2) high TTIP loss of sample 4; 3) low energy consumption of sample 2.

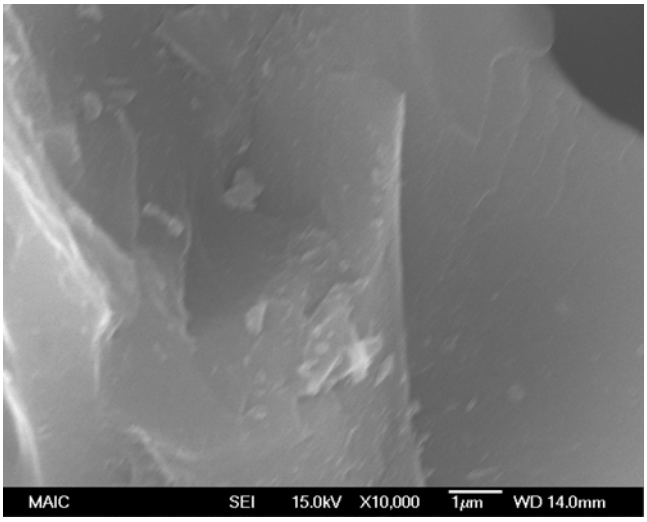

Figure 3-6 SEM image of sample 2's inner surface

Effect of TTIP Concentration

Three different TTIP concentrations (samples 2, 9, 10) were used to evaluate the effects of this parameter. Figure 3-7 shows the SEM images of the outer surface of samples 9 and 10. The SEM image of the outer surface of sample 2 is in Figure 3-4. The measured TiO_2 loading amount are listed in Table 3-1 for sample 2 and Table 3-3 for the others.

The results show that dense coating layers formed on all three samples. Therefore, TTIP concentration has no direct impact on the morphology of TiO_2. The TiO_2 loading increased with the increase of TTIP concentrations. Assuming all of the TTIP on the carbon is converted to TiO_2, the theoretical TiO_2 loading values are 8.24, 4.12, and 2.06

wt %, for 20, 10, and 5 vol % TTIP solution. Different from sample 2, the TiO_2 loadings of samples 9 and 10 were very close to the theoretical values. All TTIP converted into TiO_2 on samples 9 and 10. This is because, as discussed previously, that the hydrolysis rate was not quick enough to hydrolyze all TTIP in gas phase when the TTIP concentration was 20 vol %.

(a)

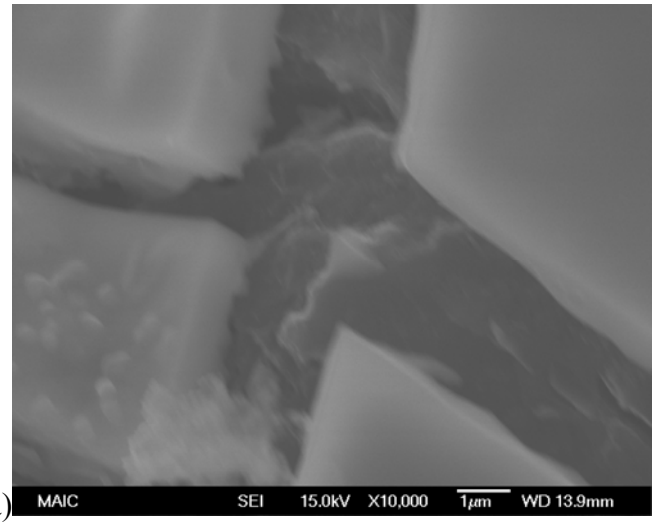

(b)

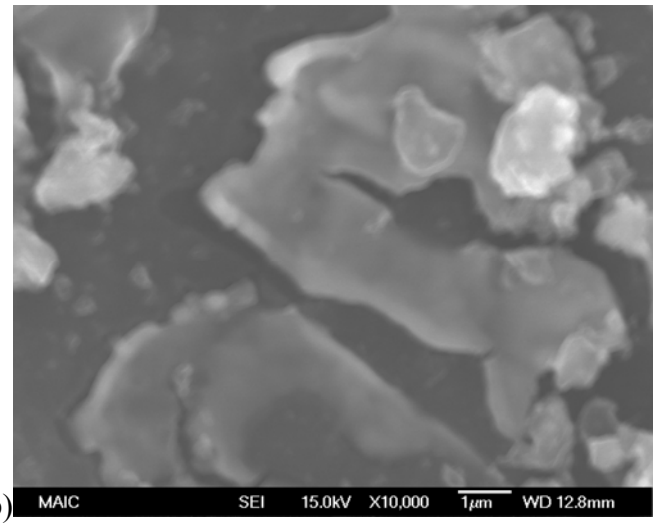

Figure 3-7 SEM images of samples 9-10. (a) sample 9; (b) sample 10.

Effect of Moisture in Carbon

Activated carbon is a good adsorbent for moisture. The AC used in samples 1- 10 was dried to remove moisture before coating. Sample 11 was prepared under the same

conditions of sample 2 except that the AC wasn't dried before coating. After heating at 105 ^{o}C for 2 h, the weight loss of the used AC was 4.73%. Because the moisture content of AC depends on the storage conditions, its value varies a lot. Figure 3-8 shows the SEM image of the outer surface of sample 11. The measured TiO_2 loading is listed in Table 3-3. Figure 3-9 shows the XRD pattern of sample 11.

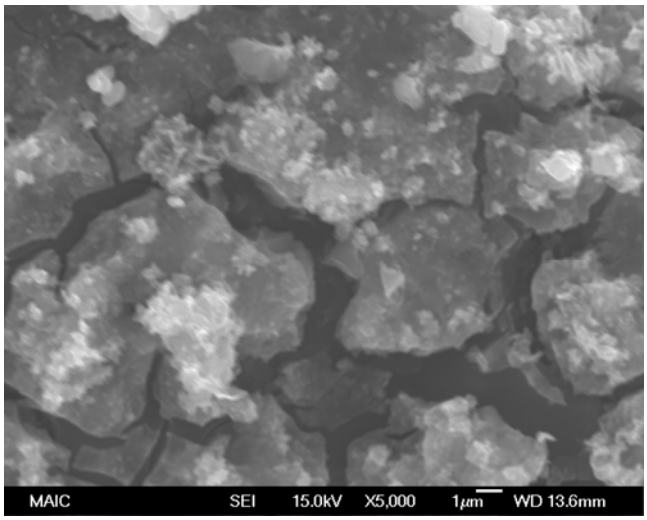

Figure 3-8 SEM image of sample 11

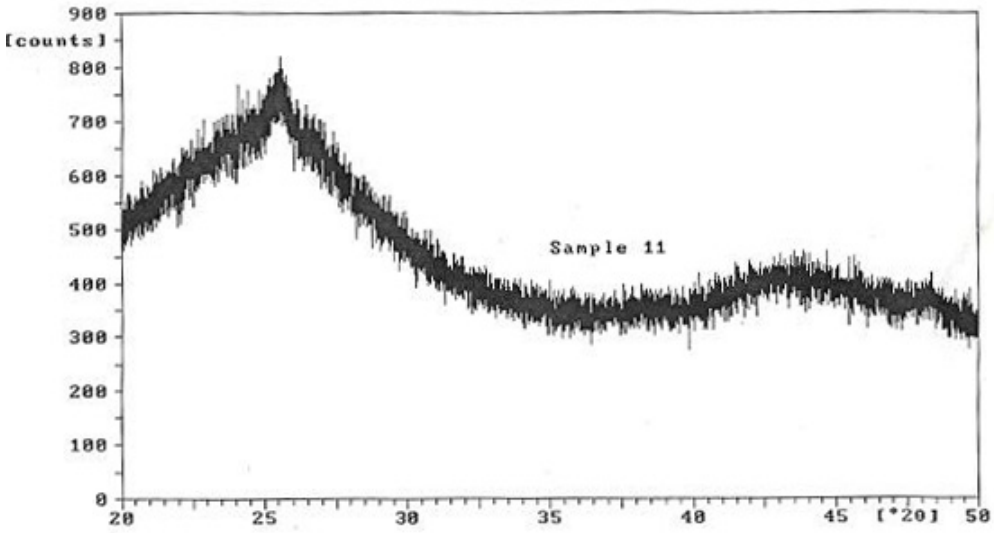

Figure 3-9 XRD pattern of sample 11

Even though the moisture hadn't been removed before impregnation, TiO_2 particles were not formed immediately after mixing with the TTIP solution. The reason is that the adsorbed water has lower reaction activity than water vapor. The TiO_2 loading of sample 2 and sample 11 were similar. Although dense coating layers formed on sample 11 (Figure 3-8), there were quite a few particles as shown. Those particles deposited on the surface of the formed dense coating layer. This indicated two kinds of hydrolysis of TTIP: 1) hydrolyzed by adsorbed water; 2) hydrolyzed by water vapor in the air streams. The TTIP hydrolyzed by adsorbed water formed the dense coating layer. The surplus TTIP hydrolyzed by water vapor in airstreams and deposited on it. Compared with the XRD patterns of sample 2 and sample 11, the moisture in the carbon increased the degree of TiO_2 crystallinity. So, it is not necessary to remove the moisture before impregnation.

Photocatalytic Activity

Methanol removal by the original AC and various TiO_2/AC composites with and without UV light was carried out in order to compare their ability to remove methanol via simultaneous adsorption and oxidation. The effluent methanol concentration profiles are shown in Figure 3-10 for the virgin AC and sample 4 as a representative. The effluent methanol concentration increased quickly when treated by the virgin AC with and without UV light. When treated by sample 4 without UV light irradiation, a similar adsorption profile was observed, and the methanol adsorption capacities for the virgin AC and sample 4 composite were similar. However, when methanol was treated by sample 4 with UV light irradiation, the methanol concentration didn't reach saturation for the duration of the experiment. The methanol concentration increased during the first 2 h and then maintained at about 58% removal. Figure 3-11 shows the methanol removal efficiency for the different TiO_2/AC samples based on the measurements of the last four h

(i.e., after the value did not vary more than 2 ppm), wherein, 9% P25/AC was Bio-Nuchar AC coated with 9 wt % P25 by spray desiccation.

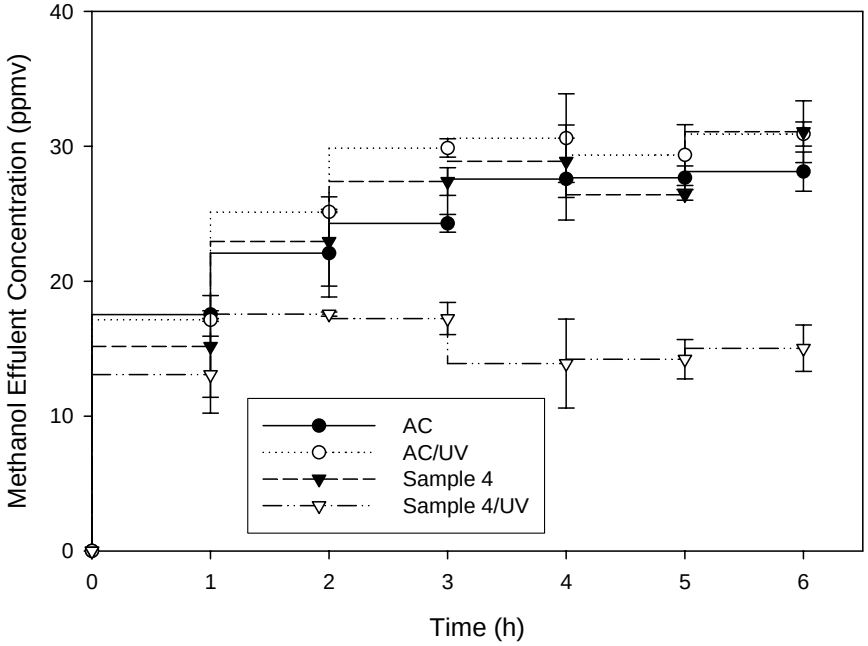

Figure 3-10 Methanol effluent concentration profiles (C_0=31.0 ppmv)

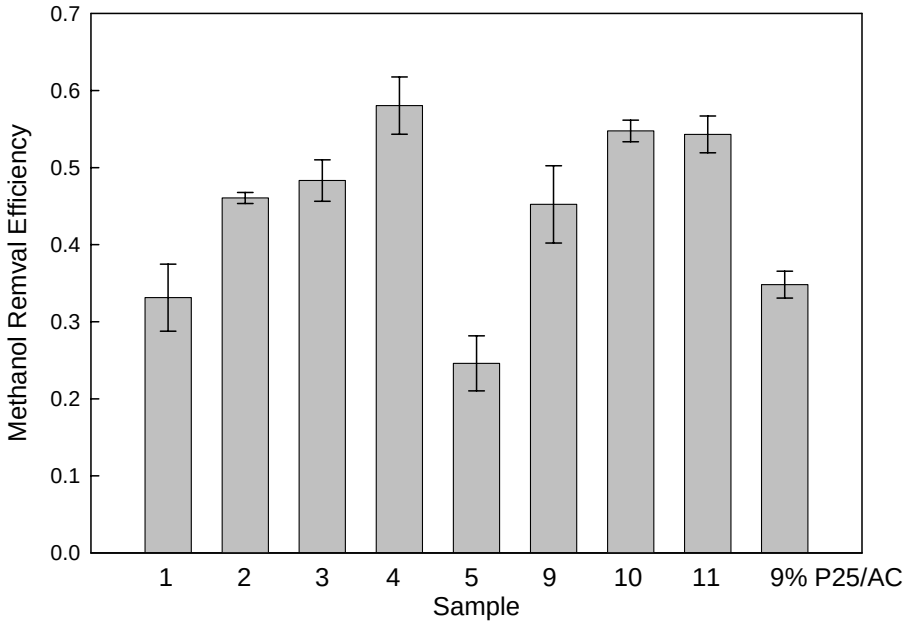

Figure 3-11 Average methanol removal efficiency of samples (C_0=31.0 ppmv)

Because of the low surface area of dense coating layer compared with particulate coating layer, photocatalytic activity of samples 1, 2, 3 and 5 was lower than that of sample 4. The TiO_2 loading also played an important role. For those samples with a dense coating layer, the photocatalytic activity was negatively correlated to the TiO_2 loading. It is well known that the photocatalytic activity decreases with the increase of particle size due to quantum size effect (Alberici et al., 1997). Although sample 5 had a higher degree of anatase crystallinity than did samples 1, 2 and 3, its methanol removal efficiency was the lowest because of the increase in the film thickness. Furthermore, it can be conjectured that the photocatalytic activity can be further improved by reducing the TiO_2 loading to a critical value. Below this critical value, the photocatalytic activity would decrease because the TiO_2 loading is too low to cover all surfaces.

The methanol removal performances of sample 2 (20 vol % TTIP) and sample 9 (10 vol % TTIP) were similar. The methanol performance of sample 10 (5 vol % TTIP) was better because of lower TiO_2 loading than those two samples. Under the same hydrolysis and calcination conditions, the TTIP concentration only influence the TiO_2 loading and had no significant effect on the TiO_2 morphology. As mentioned above, dense coating layers were formed on these three samples and photocatalytic activities were similar. Considering the effective usage of TTIP, lower concentration was preferred.

The photocatalytic activity of sample 11 was better than that of sample 2 because of the degree of TiO_2 crystallinity. Comparing sample 4 and sample 11, their methanol removal efficiencies were similar. Sample 11 was therefore used in Chapter 4 due to its high performance and simplicity in preparation procedure.

In comparison, the methanol removal efficiency of the base line (9% P25/AC) was lower than samples 2, 3, 4, 9, 10, and 11. The better distribution of TiO_2 particles prepared by the dry impregnation contributes to the better performance. The results demonstrate that the dry impregnation can be an effective method for preparing the photocatalytic TiO_2/AC composites that have a higher photocatalytic activity for methanol removal.

Conclusion

TiO_2/AC composites were successfully prepared by the described dry impregnation. TTIP was effectively converted to the anatase form of TiO_2 by hydrolysis and calcination. The hydrolysis conditions influenced the loading and morphology of the formed TiO_2. The favorable hydrolysis condition to form particulate coating layer was high temperature that would result in a concentration exceeding the critical nucleation concentration. The favorable calcination condition was 300 ^{o}C in air for 2 h. The TiO_2 was mostly coated on the outer surface and macropores of AC. High hydrolysis temperature results in particulate coating layer and high TiO_2 crystallinity. Under the same hydrolysis and calcination conditions, the TTIP concentration mainly affected the TiO_2 loading and had little influence on the photocatalytic activity. It is not necessary to remove moisture from carbon before coating. The moisture in the carbon increased the crystallinity of TiO_2. Under proper preparation conditions, the TiO_2/AC composite prepared by dry impregnation outperformed the TiO_2/AC composite prepared by spray desiccation.

CHAPTER 4
H_2S REMOVAL BY A TiO_2/AC COMPOSITE PHOTOCATALYST PREPARED BY DRY IMPREGNATION

Introduction

Properties of H_2S and Regulations

Hydrogen sulfide (H_2S) is a highly toxic air pollutant which has been identified in the list of 190 air toxic substances in Title III of the 1990 Clean Air Act Amendments (Yang, 1992). It is almost as toxic as hydrogen cyanide (HCN). Human exposure to low concentration of H_2S in air can cause headaches, nausea, and eye irritation, and higher concentration can cause paralysis of the respiratory system, which results in fainting and possibly death. Concentrations of the gas approaching 0.2% (2000 ppmv) are fatal to humans after exposure for a few minutes. Hydrogen sulfide is an odorous gas, and its presence at low concentrations is easily perceived and recognized due to its characteristic odor of rotten eggs. H_2S is perceptible to most people at the concentration in excess of 0.5 parts per billion (ppb) in air. However, as the level of H_2S increases, a person's ability to sense dangerous concentration by smell is quickly lost. If the concentration is high enough, unconsciousness will come suddenly, followed by death if there is no prompt rescue (Yang, 1992). The Occupational Safety and Health Administration (OSHA) Permissible Exposure Limit (PEL) for General Industry as follows:

> Exposure shall not exceed 20 ppm (ceiling) with the following exception: if no other measureable exposure occurs during the 8-hour work shift, exposures may exceed 20 ppm, but not more than 50 ppm (peak), for a single time period up to 10 mintes.

The National Institutes of Occupational Safety and Health (NIOSH) recommends a

single 10-ppm 10-minute ceiling PEL for this substance. Control of H_2S emissions is essential to the protection of public health and welfare as well as to the mitigation of vegetation and material damage problems (Yang, 1992).

Hydrogen sulfide is one of the major pollutants in air emissions from kraft pulp mills. It is a colorless gas, slightly heavier than air, and moderately soluble in water. The solubility of H_2S decreases with increasing temperatures. The dissolved H_2S dissociates in accordance with the following reversible ionization reactions (Yang, 1992):

$$H_2S \leftrightarrow HS^- + H^+ \quad (4\text{-}1)$$

$$HS^- \leftrightarrow S^{2-} + H^+ \quad (4\text{-}2)$$

The dissociation of H_2S is effected by pH. The concentration of HS^- species is insignificant when pH values are less than 6, and S^{2-} may not occur at all when pH values are less than 6.

Processes that have been used to remove H_2S from waste gas streams involve either physical treatment or chemical oxidation. The means of removing H_2S depend on the concentration. At high concentrations, the Claus reaction process is commonly used (Bouzaza et al., 2004). At lower concentrations, several processes have been developed, such as transition-metal oxides catalytic oxidation (Li et al., 1997), bifunctional redox scrubbing process (Petre and Larachi, 2005), and AC adsorption/oxidation (Katoh et al., 1995; Bagreev et al., 2001; Bandosz, 2002; Le Leuch et al., 2003; Bouzaza et al., 2004). Some methods require additions of chemicals, and energy expenditure is usually necessary for physical treatment. Additional environmental problems are encountered with chemical additives, where the resulting products and by-products require further treatment and disposal (Yang, 1992).

H_2S Adsorption/Oxidation on AC

Activated carbons used for the removal of H_2S are generally impregnated with caustic materials such as NaOH or KOH, or are otherwise modified. Air currents around odor-generating facilities are initially washed in scrubbers, during which they intake high levels of humidity, and are then blown through the AC vessels. The carbon bed is mostly used as a passive support for the caustic material. The disadvantages of caustic carbons include: 1) the impregnation decreases the ignition temperature of the carbon and poses a hazard of self-ignition; 2) the oxidation product is elemental sulfur which cannot be removed from carbon by washing with water; 3) the activity of caustic carbons toward H_2S oxidation ends when the caustic is consumed and the carbon pores are blocked by sulfur and sodium or potassium salts; 4) its cost is much higher than virgin AC (Bandosz, 2002).

The application of virgin (unimpregnated) AC for the removal of H_2S from air has been investigated. Many papers published in the literature indicate a good removal efficiency of H_2S on ACs (Katoh et al., 1995; Bagreev et al., 2001; Bandosz, 2002; Le Leuch et al., 2003; Bouzaza et al., 2004). The structural parameters and surface chemistry of ACs, which are governed by the presence of heteroatoms (such as oxygen, hydrogen, nitrogen, sulfur, and phosphours), are important for their performance as a H_2S remover. The surface area and pore volume are not the crucial factors that determine the final performance of carbons as H_2S removers (Bandosz, 2002).

The pH of carbon surface has a significant effect on the efficiency of H_2S dissociation and its oxidation to various sulfur species. A moderately low average pH of the carbon surface is expected to suppress the dissociation of H_2S and the creation of HS^- ions. Hydrosulfide ions, when present in low concentration on carbon surface are

oxidized to sulfur oxides which subsequently form sulfuric acid. When the pH value is very low (< 4.5), only physical adsorption can occur and the concentration of dissociated H_2S ions is negligible. On the other hand, a pH in the basic range promotes the dissociation of H_2S. This results in a high concentration of HS^- ions, which are then oxidized to sulfur. For the efficacy of regeneration of the spent carbon, the formation of sulfuric acid is preferred. Water is another important factor in the process of H_2S removal. The data collected by Bandosz clearly show that the H_2S breakthrough capacities of prehumidified carbons are about two to six times higher than those of the as received carbons (Bandosz, 2002). The presence of humidity in airstreams increased strongly the equilibrium capacity (in batch reactor) of ACs compared to dry atmosphere (Le Leuch et al., 2003). However, an excess of water flooding was reported as a factor that decreased adsorption of H_2S on AC. The optimal relative humidity for WWP3 AC cloth was around 60% (Le Leuch et al., 2003).

When H_2S is adsorbed onto unmodified ACs at elevated temperatures, elemental sulfur is the main product. Elemental sulfur also deposits when caustic carbons are used. At ambient temperature, however, sulfuric acid is formed and results in a significant decrease in the pH of carbon (Bandosz, 2002). The mechanism of H_2S oxidation on AC proposed by Hidden et al. (1976) requires the presence of a water film, which enables the dissociation of H_2S molecules to HS^- ions. The following figure shows the proposed pathway of H_2S oxidation on unmodified AC (Bandosz, 2002).

Under dry air, Le Leuch et al. (2003) proposed the mechanism of H_2S oxidation on AC as follows:

$$2C_f + O_2 \rightarrow 2C(O) \qquad (4\text{-}3)$$

$$H_2S + C(O) \rightarrow \frac{1}{8}S_8^{\ 0} + H_2O + C_f \qquad (4\text{-}4)$$

where C_f is free active site, maybe an oxygen-containing site or radical C formed at the carbon surface. The first mechanism is the adsorption of oxygen from air by the carbon. The second mechanism is the oxidation of H_2S by the adsorbed oxygen.

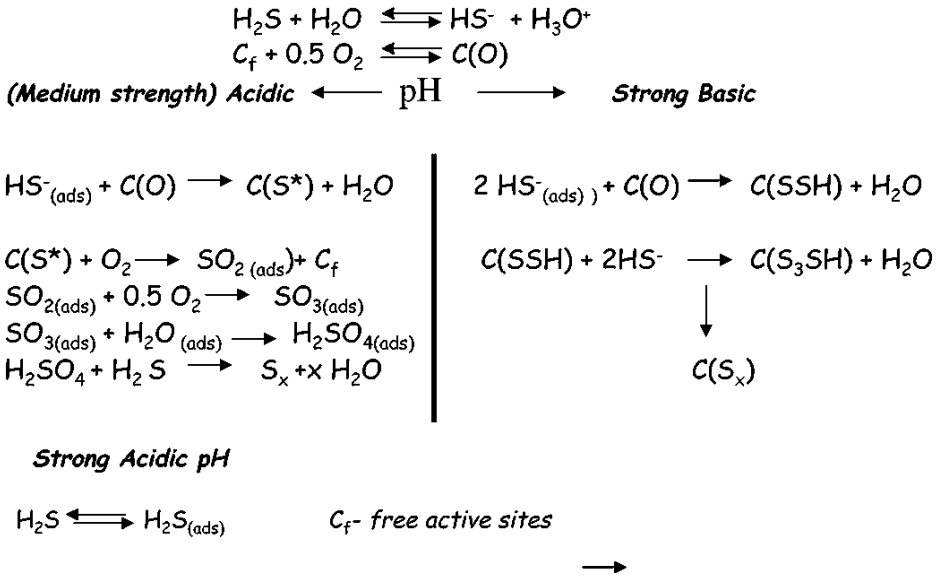

Figure 4-1 Proposed pathway of H_2S oxidation on unmodified AC in the presence of water (Bandosz, 2002)

Bandosz (2002) investigated the regeneration of the exhausted carbon by water washing or heat treatment. The study of the water regeneration showed that after the first adsorption run around 60% capacity was lost irreversibly. This was the result of the deposition of elemental sulfur in carbon micropores and the strong adsorption of sulfuric acid leading to the low pH. The regeneration of spent carbon by heating at 573 K resulted in 70% capacity loss.

The H_2S destruction in gas-phase using TiO_2 photocatalyst has been studied by Canela et al. (1998). These authors observed high degradation yields of 99% at concentration of 33 to 855 ppmv. Oxygen was shown to be necessary for the

photodestruction of H_2S. The photocatalytic process using TiO_2/UV-VIS showed that at 217 ppmv, there was no loss of the activity over extended operation periods (3 h). The main product in the photocatalytic destruction of H_2S in gas-phase was sulfate ions.

The objective of this chapter was to evaluate the performance of the TiO_2/AC composite photocatalyst developed in the previous chapter as a H_2S remover. Although H_2S is among the pollutants effectively removed by AC (Bagreev et al., 2001), TiO_2/AC composite was used to increase the oxidation of H_2S to sulfate.

Experimental Section

Materials

All chemicals were reagent grade or better: H_2S/air mixture (1000 ppmv, Praxair); DI water (> 17.9 MΩ/cm); air (breath grade, Praxair). AC used in this study was MeadWestvaco Bio-Nuchar 120 (a chemically activated wood based carbon, 8 – 12 mesh). The TiO_2/AC composite photocatalyst used was Sample 11 prepared by dry impregnation method as described in Chapter 3.

Photocatalytic Activity Evaluation

Figure 4-2 shows the experimental set-up. The H_2S (1000 ppm in air) from a cylinder was mixed with air and diluted to around 40 ppm. The reactor was the same as in Chapters 2 and 3. The temperature of the reactor was measured by the thermal couple inserted in the reactor. Each time 1.00 g adsorbent was used. The flow rate was 0.42 L/min and the EBCT was 0.35 s. The H_2S removal was tested with UV light and without UV light (at room temperature). Because the reactor has no cooling system, the temperature rises to 328±2 K when the UV light is turned on. The H_2S removal by AC at 328 K was also carried out to investigate the effect of temperature (the UV lamp was covered by Al foil and turned on so that there was no UV light in the reactor but the

temperature was the same as the run with UV light). For convenience, the labels RT (at room temperature, without UV), 328 K (at 328 K, without UV), and UV (under UV Light irradiation) were used to indicate the experimental conditions.

A Jerome 631-X H_2S analyzer (Arizona Instrument LLC) was used to measure H_2S concentrations in the sample gas. The detection range of the analyzer is 0.003 to 50 ppm and the precision is 5% relative standard deviation. H_2S concentration at the inlet of the reactor was measured when the H_2S laden gas bypassed the reactor. By comparing the outlet H_2S concentration with the inlet level, the H_2S removal efficiency can be obtained. Finally, the gas stream passed through an alkaline trap before it was exhausted into the fume hood. The amount of sulfate formed on the adsorbents was measured according to the following method. The used sample was taken out and added to 100 ml DI water (> 17.9 MΩ/cm) and the suspension was stirred overnight to reach equilibrium (Bandosz, 2002). In the following morning, the sample was filtered and the sulfate concentration in the filtrate was measured by ion chromatography (ICS-1500, DIONEX).

The H_2S removal efficiency and sulfate conversion efficiency were calculated according to the following equations:

$$n_t = \frac{C_i \times Q \times t}{24.5} \tag{4-5}$$

$$n_r = \frac{\sum \frac{(C_i - C_t)}{2} \times \Delta t \times Q}{24.5} \tag{4-6}$$

$$\eta_r = \frac{n_r}{n_t} \times 100\% \tag{4-7}$$

$$\eta_c = \frac{n_s}{n_r} \times 100\% \tag{4-8}$$

where, n_t (mol) is the total H_2S amount entering the reactor; C_i (ppm) is the inelt concentration of H_2S; t (min) is the total time of experiment; Q (L/min) is the gas flow rate; 24.5 (L/mol) is the gas constant at 25 ^oC and 1 atm; n_r (mol) is the removed H_2S amount during the experiment; C_t is the outlet concentration of H_2S at time t; Δt (min) is the time interval between two data points; n_s (mol) is the amount of sulfate formed on the adsorbent; η_r is the H_2S removal efficiency; η_c is the sulfate conversion efficiency.

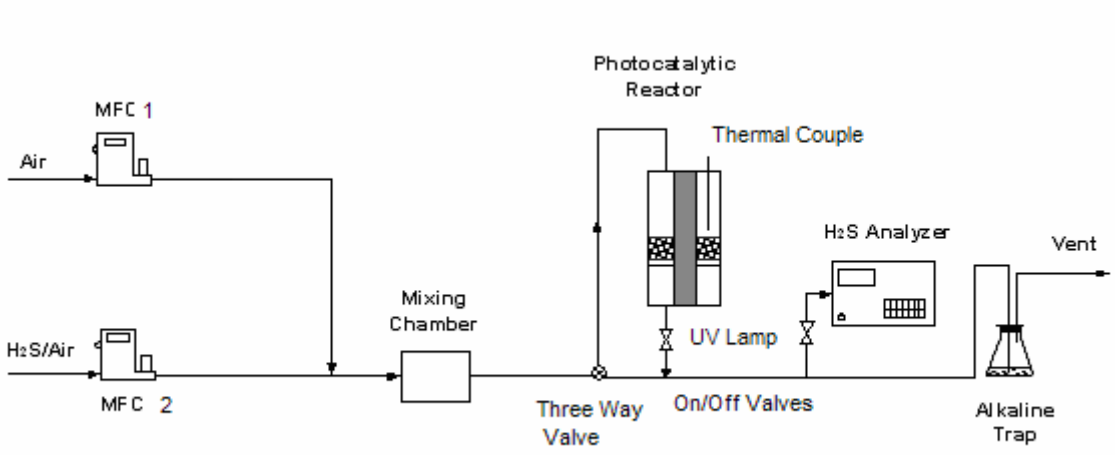

Figure 4-2 Experimental set-up for H_2S removal

Results and Discussion

Figure 4-3 shows the outlet concentration profiles of virgin BioNuchar AC and TiO2/AC in dry condition. From bottom to top, the six lines are AC/UV, AC/328K, AC/RT, TiO_2/AC/UV, TiO_2/AC/328K, and TiO_2/AC/RT respectively. In all cases, the outlet H_2S concentration increased with time and was lower than the inlet concentration during the entire operation period (120 min), indicating that the adsorbents were not saturated. Hence, the removal amount calculated by Eq. 4- 6 was not the saturation capacity. The outlet concentrations of TiO_2/AC were higher than that of AC in all three conditions. Figure 4-4 shows the H_2S removal efficiency and sulfate conversion efficiency in each situation. For AC, the removal efficiencies were 91.40 ± 1.84 % (RT),

96.84 ± 0.65 % (328 K), and 97.97 ± 0.10 % (UV); the sulfate conversion efficiencies were 15.01 ± 1.93 % (RT), 12.57 ± 1.66 % (328 K), and 14.10 ± 2.15 % (UV). For TiO_2/AC, the removal efficiencies were 45.70 ± 5.64 % (RT), 53.78 ± 0.32 % (328 K), and 86.62 ± 1.93 % (UV); the sulfate conversion efficiencies were 13.45 ± 4.37 % (RT), 12.11 ± 0.39 % (328 K), and 18.73 ± 1.24 % (UV). Details of the effect of each parameter are discussed below.

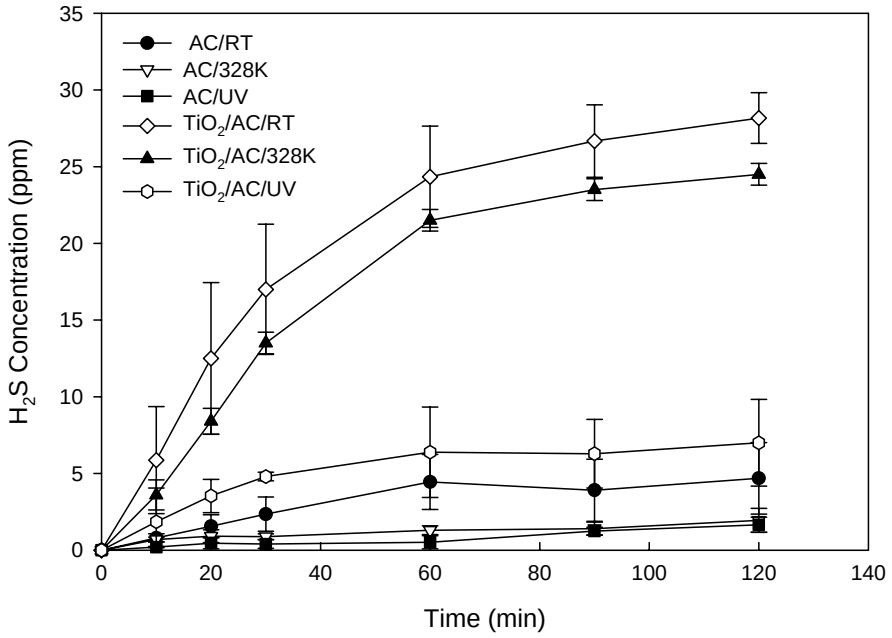

Figure 4-3 Outlet H_2S concentration profiles (inlet concentration was 40.5 ppm, RH = 0%)

Surface pH As shown, BioNuchar AC is a better H_2S remover than TiO_2/AC. This may result from the changes of the surface properties during the preparation. As discussed earlier, the surface chemistry is the dominant factor in the H_2S removal performance of carbons. The pH of carbon surface has a significant effect on the removal capacity of H_2S. To verify the effect of this parameter, the pH of the virgin BioNuchar AC and the TiO_2/AC composite were measured. 0.4 g of dry sample was added to 20 ml

of DI water (> 17.9 MΩ/cm) , and the suspension was stirred overnight to reach equilibrium (Bandosz, 2002). The sample was then filtered and the pH of the filtrate was measured by Accumet AP71 pH meter. The results are listed in Table 4-1.

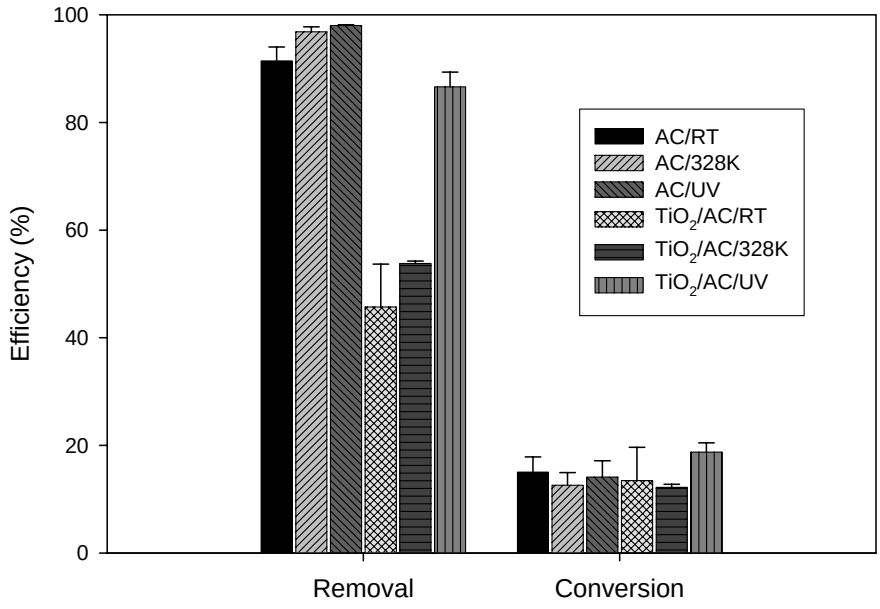

Figure 4-4 H_2S removal efficiency and SO_4 conversion efficiency (inlet concentration was 40.5 ppm, RH = 0%)

Table 4-1 Surface pH of AC and TiO_2/AC

Sample	Surface pH
BioNuchar AC	6.84±0.13
TiO_2/AC	4.19±0.36

The virgin BioNuchar AC has a moderate pH which is good for both high capacity and sulfuric acid formation (Bandosz, 2002). After coating TiO_2, the surface pH was decreased to acidic range which is not desired for H_2S removal.

Temperature High temperature improved the H_2S removal on AC and TiO_2/AC. Generally, chemical reaction proceeds faster at higher temperature. The oxidation of H_2S on AC was faster at 328 K than at room temperature. Therefore the removal efficiency increased. The sulfate conversion efficiencies at 328 K decreased compared to at room

temperature. As mentioned above, elemental sulfur is the main product of H_2S oxidation on unmodified AC at elevated temperature (Bandosz, 2002).

UV light At the same temperature (at 328 K), UV light irradiation improved the H_2S removal on TiO_2/AC from 53.78 % to 86.62%. Furthermore, sulfate conversion efficiency, which is important for regeneration using water wash, was also increased. This proved that H_2S was photocatalytically degraded on TiO_2/AC composite. Compared to the results of Canela et al. (1998), the H_2S removal efficiency and sulfate conversion efficiency of TiO_2/AC with the presence of UV light are lower. This is mainly because the EBCT was much shorter (0.35 s) in the current system. The EBCT used by Canela and coworkers was 48 s.

UV light also improved the removal of H_2S on AC. In Figures 4-3, the outlet H_2S concentration of AC/UV was lower than that of AC (328 K). The difference between AC/UV and AC (328 K), however, was not clear because the removal efficiencies in both cases were high. To clarify the effect of UV light, H_2S was increased to 59 ppm. It should be noted that the inlet concentration was calculated according to the flow rates of the two mass flow controller and the H_2S concentration in the cylinder because the inlet concentration was out of the measuring range of 631X H_2S analyzer. Figure 4-5 shows the removal and conversion efficiencies.

With the increase of inlet H_2S concentration to 59 ppm, the removal efficiencies decreased to 85.03 ± 5.07 % (RT), 88.77 ± 3.78 % (328 K), and 94.75 ± 1.96 % (UV) respectively. The difference between AC at 328 K and under UV irradiation was increased. This proved that UV light improved the AC performance. The sulfate conversion efficiencies were 15.72 ± 1.87 % (RT), 20.03 ± 1.19 % (328 K), and 15.14 ±

0.12 % (UV). Except at 328 K without UV irradiation, the sulfate conversion efficiencies were almost the same as the case of 40.5 ppm inlet concentration. The peak wavelength of the used UV lamp (black light lamp) is 365 nm. Photolysis of H_2S occurs in light with wavelength shorter than 300 nm (Khriachtchev et al., 1998). However, Nozawa et al. (2001) observed the photolysis of H_2S under black light lamp (365 nm). This was inconsistent with the results of Khriachtchev and co-workers (1998). Figure 4-6 shows the relative outlet concentration of H_2S under UV light irradiation without AC or TiO_2/AC adsorbent (i.e. empty reactor).

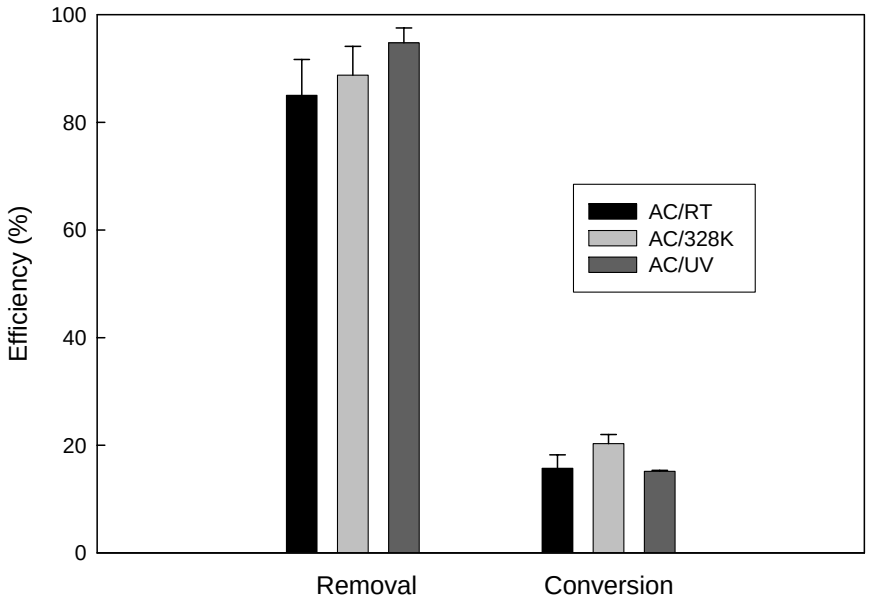

Figure 4-5 H_2S removal efficiency and SO_4 conversion efficiency of AC (inlet concentration was 59 ppm, RH = 0%)

The outlet concentration was lower than the inlet concentration. This might result from the H2S adsorption on the reactor (reactor wall, porous frit, and tubing). With the presence of UV light, the outlet concentration was not lower than that without UV light. After 30 minutes, the outlet concentration with the presence of UV light was higher than

that without UV light because of the rise of temperature and decrease of adsorption. The results proved there was no photolysis under the black light lamp used (365 nm). Therefore, photolysis is not responsible for the improved H2S removal on AC under the UV light in the current system (365 nm). There are two possible mechanisms for the enhanced removal and conversion of AC under UV. It is possible that UV light induces heterogeneous photolysis of H2S adsorbed to the external surface of the carbon. Another possible mechanism is the functional groups of AC, such as carbonyl group, are excited under UV light irradiation. The mechanism wasn't further explored due facility limitation. To the best of the author's knowledge, this phenomena and mechanism have not been reported

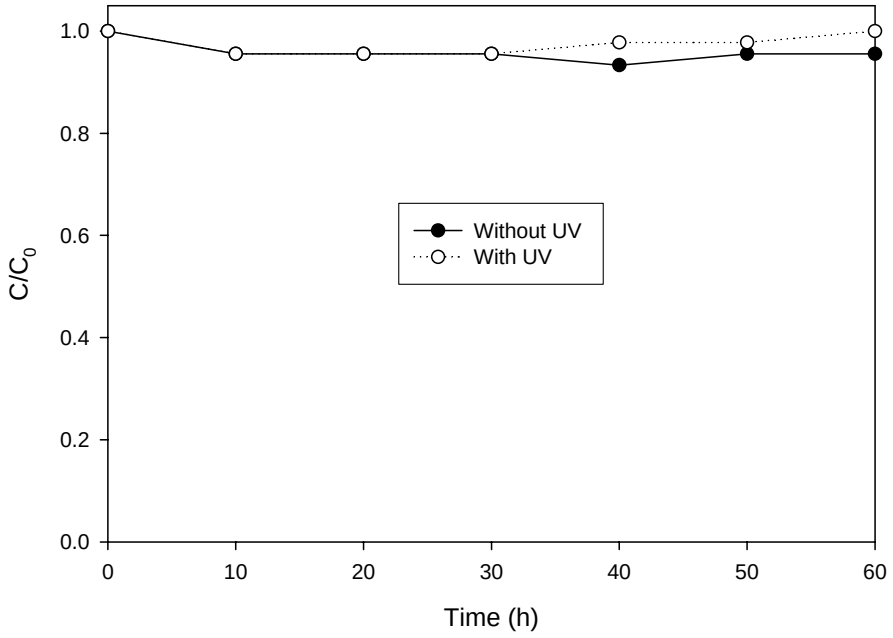

Figure 4-6 Outlet H_2S concentration passing empty reactor (inlet concentration was 45 ppm, RH = 0%)

Conclusions

BioNuchar AC itself is a good H_2S remover. Without UV irradiation, a fraction of adsorbed H_2S was already oxidized to sulfate. The presence of UV light improved H_2S removal efficiency in dry airstreams. After coating TiO_2, the H_2S removal efficiency of TiO_2/AC decreased due to the surface change. Under UV light irradiation, H_2S removal efficiency and sulfate conversion efficiency of TiO_2/AC composite increased. The sulfate conversion efficiency of TiO_2/AC composite was higher than that of AC which is preferred for water regeneration.

CHAPTER 5
MICROWAVE-ASSISTED PREPARATION OF TiO_2/AC COMPOSITE PHOTOCATALYST

Introduction

Microwave is a form of energy that falls at the lower frequency end of the electromagnetic spectrum. It is defined in the 300 to 300,000 megahertz (MHz) frequency range. A microwave is comprised of two elements: an electric field and a magnetic field (Figure 5-1). Microwave was first developed primarily for communications. Around 40 years ago, the heating effect of microwave was discovered. Microwave, as a heating method, is a dielectric heating method using dipole rotation and ionic conduction, wherein the applied energy is converted into heat by mutual interaction between media. In contrast to all other commonly used heating methods, microwave allows volumetric heating of materials. Processes based on microwave heating find many industrial applications such as cooking, tempering and thawing, and curing of wood and rubber products.

The electromagnetic energy of microwaves is dissipated by substances through three different mechanisms (Bathen, 2003):

- Magnetic losses in ferromagnetic materials;
- Ohmic losses in conducting materials;
- Electric losses caused by electromagnetic inhomogeneities like dipoles and ions.

The following explains the mechanism of electric loss. The electric field of microwave interacts with molecules through either a dipole or ionic conductivity in the molecules themselves. As the electric field changes from positive to negative, the positive

and negative ends of the dipole (or the positive and negative ions) seek to align with the opposite field. This causes molecular rotation (Figure 5-2). The rotational motion of the molecule as it tries to orient itself with the field results in transfer of energy. The coupling ability of this mechanism is related to the polarity of the molecules and their ability to align with the electric field. There are a number of factors that will ultimately determine the dipole rotation coupling efficiency; however, any polar species (solvent and/or substrate) present will encounter this mechanism of energy transfer.

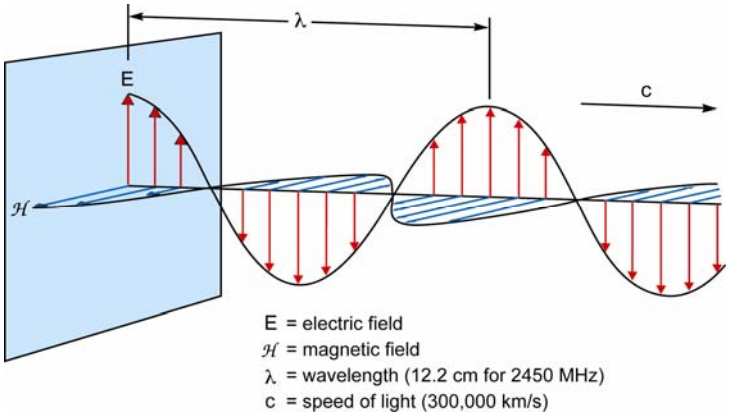

Figure 5-1 Schematic description of a microwave (Hayes, 2002).

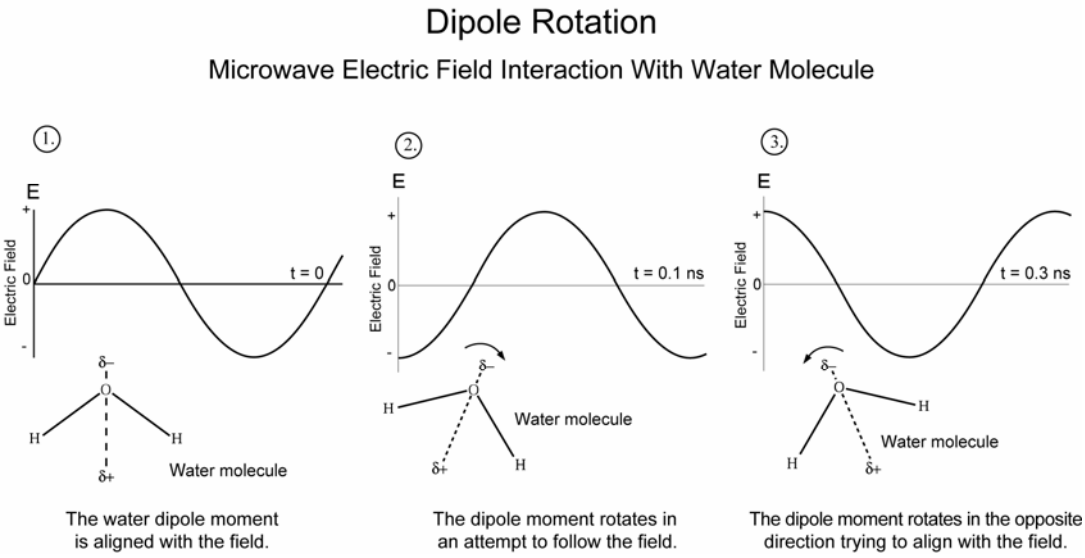

Figure 5-2 Rotation of molecules with microwave (Hayes, 2002).

Of the four frequencies available for industrial, scientific, or medical applications (915 MHz, 2450 MHz, 5800 MHz, and 22,125 MHz), 2450 MHz is the most commonly used. At this frequency, the energy supplied to the system is equal to 0.037 kcal/mol. Even the weakest intramolecular bonds (Van der Waals forces) are 48 kcal/mol. Therefore, microwave only serves to rotate the molecules, and will neither break nor form any additional bonds. (Hayes, 2002)

Materials like glass, octane or nitrogen (with none of the properties mentioned earlier), are transparent to microwave. Microwave energy transfer is not dependent on thermal conduction and is very rapid, e.g. heating water in a beaker. With conventional (conductive) heating, as a hotplate is slowly heated, thermal energy is slowly transferred to the beaker. That heat must then be transferred again through each layer of water until the temperature is uniform. Microwave transfers energy differently. Glass vessels are transparent to microwave energy, enabling the water molecules to absorb the energy directly, meaning more efficient energy transfer. As a consequence, thermal energy is produced only as a byproduct (Hayes, 2002).

The property that describes how well a material absorbs microwave energy and converts it into heat is the dielectric loss factor (ε''). In general, the heat-up rate of a material in an applied electric field is proportional to the dielectric loss factor, frequency, and the square of the strength of the electric field inside the material. The penetration depth (δ), defined as the distance from the surface of the bed at which the power decay to 1/e of its value at the surface, is inversely proportional to the dielectric loss factor (Bathen, 2003) as

$$\delta = \frac{\lambda_0 \sqrt{\varepsilon'}}{2\pi\varepsilon''} \qquad (5\text{-}1)$$

where λ_0 is the wavelength of the radiation in free space, ε' is the dielectric constant, and ε'' is the dielectric loss factor. This equation suggests that a material with a high loss-factor, such as activated carbon, exhibits short penetration depths, making it difficult to uniformly heat a large bed of the material. Table 5-1 lists some calculated values according to the above equation (Bathen, 2003).

Table 5-1 Penetration depth of microwaves (2.45 GHz)

Compound	Temperature (^oC)	Penetration depth (cm)
Air	25	infinity
Water (distilled)	25	1.42
Water with 29 g/l NaCl	25	0.38
Methanol	25	0.64
Tetrachlorocarbon	25	3210
Zeolite NaX	20	15.71
Zeolite DAY	20	>100
Aluminum	25	0.02
Aluminum Oxide	25	656

Advantages of microwave heating include (Bykov et al., 2001):

7. Reducing energy consumption and process time: microwave energy transforms into heat inside the material, which results in significant energy savings and reduction in process time.

8. Rapid and controllable heating: the heat is transmitted directly inside the sample, and the heating rate is controlled by the power of the microwave source.

9. Inverse temperature profile: the heat is dissipated to the environment through the surface. Therefore, the temperature inside the sample is always higher than on the surface (including the case when a constant temperature is maintained). In order to reduce this temperature difference the sample can be surrounded by a layer of a thermally insulating material which reduces heat loss from the surface of the sample.

10. Selectivity: microwave heating is based on the capacity of a material to absorb the electromagnetic energy. The selective absorption of microwave irradiation opens a way to implementation of selective heating.

11. Possibility of surface processing: for a given material and frequency, if the microwave penetration depth is small enough, microwave heating takes place only in the near surface layer of the material.

Besides these advantages, there are many experimental observations that suggest non-thermal microwave effects that accelerate reaction rates, alter reaction pathways, and enhance mass transport and result in unique properties in polymers, ceramics and composites. Still, the specific mechanism of this effect needs further theoretical and experimental investigation (Bykov et al., 2001).

There are several reports in the literature of TiO_2 powder preparation by microwave processing. Ramakvishnan (1999) synthesized titania ceramic powders from TTIP in methanol under microwave irradiation. Ayllón et al. (2000) prepared anatase TiO_2 powder from fluorine-complexed titanium aqueous solution using microwave irradiation. Crystalline anatase TiO_2 powders with submicron size were obtained in a short time, at low temperature and atmospheric pressure. However, the obtained materials did not show photocatalytic activity. Wilson et al. (2002) reported microwave hydrothermal treatment of colloidal TiO_2 suspensions. Their results showed that the microwave treatment allowed for rapid heating rate and rapid recrystalization. This resulted in highly nanocrystalline material and reduced process time and energy with respect to the conventional hydrothermal treatment. Yamamota et al. (2002) studied hydrolysis and polycondensation of TTIP in alkanedial solvent under microwave irradiation to obtain anatase TiO_2 nanocrystallite. Hart et al. (2004) synthesized anatase TiO_2 by a sol-gel method followed by microwave heat treatment (silicon carbide was used as a microwave susceptor). Using microwave processing, crystallization of TiO_2 was significantly faster and occurred at lower temperature than by conventional furnace treatments. While there have been many studies on the preparation of TiO_2 powder by microwave processes, there are only few

literature relevant to the preparation of TiO_2/AC by microwave process. Lee et al. (2004) reported the preparation of TiO_2/AC by a modified sol-gel method followed by drying and microwave heat treatment. The prepared material successfully degraded microcystin-LR in water. However, they simply used microwave in the heat treatment to accelerate crystallization without taking advantage of enhanced chemical reactions.

The objective of this chapter was to prepare dispersed TiO_2 photocatalyst on AC via microwave-assisted impregnation method for the treatment of HVLC emissions from paper and pulp mills. Methanol was chosen as the target pollutant because it is the major pollutant in the HVLC emissions. With microwave heating, the microwave supply energy to the carbon particles themselves. Some carbons have free electrons whose displacement is restricted by grain boundaries. When these carbons are subjected to the electromagnetic field of microwave, space charge polarization takes place. Entire macroscopic regions of the material become either positive or negative synchronizing their orientation with the field. This mechanism is often called the Maxwell-Wagner effect. At low frequency the polarization synchronizes its orientation with the field, but as the frequency increases there is a phase lag between the polarization of energy and heating of the carbon particles (Carrott et al., 2001). One advantage of microwave-assisted preparation of TiO_2/AC is the use of AC as the microwave susceptor. In this way, heat-enhanced processes such as desorption, hydrolysis, and crystallization are favored, eventually leading to quick formation of crystallized TiO_2.

Experimental Section

Materials

All chemicals were reagent grade or better: Titanium tetra-isopropoxide (TTIP) ($Ti(OC_3H_7)_4$, 98+%, Fisher); 2-proponal (99.9%, Fisher); methanol/air mixture (1000

ppmv, Praxair); DI water; F400 AC (coal based thermally activated carbon, effective particle size 14-20 mesh, Calgon). F400 AC was chosen because the thermal stability of BioNuchar AC used in previous chapters was not as good as F400 AC.

TiO_2/AC Preparation

A commercial microwave oven (SHARP CAROUSEL II) was used as the microwave source. The capacity of the oven is 0.8 ft^3, the full power is 800W, and the microwave frequency is 2450 MHz. It should be noted that the microwave power output in a common microwave oven can not be adjusted. When the power level is adjusted, it merely regulates the fraction of synchronic irradiation time. At high, medium, medium low, and low power level, the fractions of synchronic irradiation time are 100%, 60%, 40%, and 20% respectively.

Before experiments, AC was dried at 383 K for 2 hours. A typical procedure of the preparation of TiO_2/AC by microwave-assisted impregnation was as follows: F400 AC (1.00 g) was impregnated with l mL 50% TTIP 2-propanol solution in a 20 mL glass vial and then stood for overnight to allow the solution to penetrate the pores of carbon. A designated amount of water was added into the vial and the vial was immediately exposed to microwave irradiation. The hydrolysis of TTIP produced a supersaturated vapor of TiO_2, which nucleated and grew to form TiO_2 particles on the AC surface. After a designated period of time, the sample was taken out and weighed. The effects of microwave power level, H_2O/TTIP ratio and irradiation time on the activity of TiO_2/AC, which were characterized by the methanol removal efficiency, were explored. Table 5-2 lists the preparation conditions.

Table 5-2 Preparation conditions and characterization of TiO_2/AC

Sample No.	MW Power	H_2O/TTIP Ratio	Irradiation Time	TiO_2 Loading (wt %)	BET Surface Area (m^2g-1)	Total Pore Volume (cm^3g-1)
12	Medium	28	20 min	8.59±0.05	753.06	0.4091
13	Medium Low	28	20 min	8.78±0.21	723.52	0.3928
14	Low	28	20 min	--	--	--
15	Medium	4	20 min	9.42±0.52	887.48	0.4561
16	Medium	28	30 min	9.27±0.12	905.19	0.4652
17	Medium	4	30 min	8.94±0.46	891.83	0.4504

Characterization

The specific surface area and pore size distribution of the carbon and TiO_2/AC samples were obtained by N_2 adsorption/desorption isotherms performed at 77 K (NOVA 2200, Quantachrome). All samples were outgassed at 393 K on the outgas station overnight prior to measurement. The specific surface area was determined by multipoint BET using the adsorption data in the relative pressure (P/P_0) range of 0.005-0.20. The isotherms were used to determine the total pore volume of different samples. The surface morphology of TiO_2/AC composites was characterized by Scanning Electron Microscopy (JSM 6330F, JEOL). The samples were also analyzed by X-ray diffraction (XRD 3720, Philips) for identification of crystalline species in the continuous-scan mode. The scanning speed was 0.05 $^o sec^{-1}$ or 0.005 $^o sec^{-1}$ and the scanning range was from 20^o to 50^o. The major anatase (101) peak at $2\theta = 25.4^o$ was analyzed. The TiO_2 loading on the AC was estimated by ash content analysis as described in Chapter 2.

Photocatalytic Activity Evaluation

As used in Chapters 2 and 3, low methanol concentration and high humidity were chosen. The experimental set up is shown in Figure 2-2. 2.00 g of TiO_2/AC was placed on the frit in the reactor. The methanol concentration in the influent and effluent of the

reactor during the experiment was measured by the same method used in Chapters 2 and 3.

The TiO_2/AC sample was humidified until equilibrium was established at a constant stream humidity (RH= 80% at 298 K, water concentration was 19 mgL^{-1}). Humidification was achieved by bubbling the carrier gas (air) through the vessel with water at the rate of 0.4 L/min. Humid methanol laden air (water concentration was 19 mgL^{-1}) was then passed through the fixed bed of TiO_2/AC with or without UV light for 6 hours. With UV light irradiation, the temperature of the reactor rose to 328 K from room temperature due to the heat release from the UV lamp and the relative humidity was 16% at 328 K. The bed depth was 0.4 cm and the empty bed contact time (EBCT) was approximately 0.35s.

Results and Discussion

Carbon Weight Loss and TiO_2 Loading

In order to investigate the stability of AC under microwave irradiation, 1.00 g virgin F400 AC was placed in a 20 mL glass vial and then exposed to microwave irradiation. After a designated period of time, it was taken out and weighed. Figure 5-3 shows the weight loss curves of F400 AC under different power levels of microwave irradiation.

The carbon did not start to combust under the tested conditions. However, the results (Figure 5-3) show that under high power level F400 activated carbon continue to lose weight in 30 minutes. Under medium power level F400 AC just lost weight in the first 10 minutes and the weight loss was much less than that under high power level. Because of the instability of F400 AC under high power level, this level was not used in subsequent study and only power levels equal to or less than medium were used. The

weight loss of F400 AC is likely due to the removal of some surface functional groups and/or the oxidation of carbon. The ash content of F400 AC before and after microwave process listed in Table 5-3 proved that the carbon lost some flammable composition in the microwave process. The pH of the carbon suspension, which provides some information about the average acidity/basicity of carbons, was measured following the procedures described in Chapter 4. The pH of F400 AC before and after microwave process are also listed in Table 5-3. The results showed the pH of carbon surface increased after microwave process. This may result from the decomposition of oxygenated surface groups. The carboxylic and lactonic functional groups on AC surface are less stable, which decompose at temperatures as low as 570 K and evolve CO_2 (Li et al., 2003). The phenol, quinine, and carbonyl groups are fairly stable, which only decompose at temperature above 770 K and evolve CO (Li et al., 2003). Li and co-wokers (2003) observed the starting decomposition of surface functional groups of AC in He flow as low as 400 K. Li et al. (2003) also reported that AC treated in air at 693 K resulted in the increase of surface area and pore volume. This proved that AC may be oxidized by air at elevated temperature.

Table 5-3 lists the ash content, BET surface area, and total pore volume of virgin F400 AC and the F400 AC after 20 minutes medium level microwave irradiation. As shown, the microwave process did not significantly affect the specific surface area and total pore volume of F400 AC. This also proved that the F400 AC was stable under medium power level irradiation. Because carbon and 2-propanol solvent are flammable, it may not be safe to run the microwave process in air, if vapor pressure is high. The explosion limits of 2-propanol are 2.0 vol % (lower) and 12.7 vol % (upper). In each

experiment, just 1 g of carbon and 1 mL of 50% TTIP solution were used. The volume percentage of 2-propanol vapor in the used microwave oven was less than 1 vol %. Hence, it was safe under medium or lower power level.

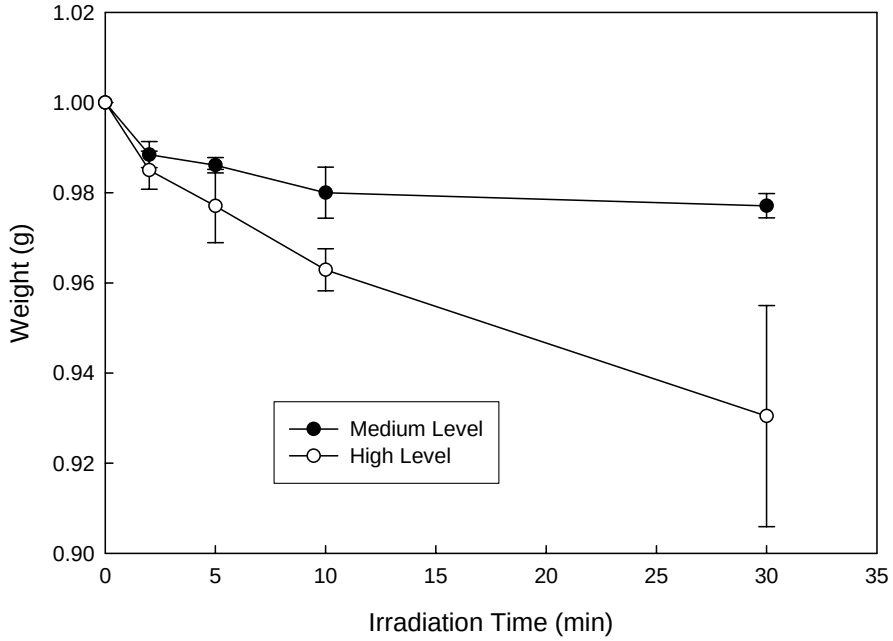

Figure 5-3 F400 AC Weight Loss under medium level MW irradiation

Table 5-3 Ash content of F400 AC before and after microwave process

	Ash Content (wt %)	BET Surface Area1 (m^2g-1)	Total Pore Volume (cm^3g-1)	Surface pH
Virgin F400	5.54±0.03	1005.10	0.5290	6.18±0.02
MW F400*	5.69±0.06	1025.19	0.5289	6.83 ±0.03

* MW F400 is virgin F400 carbon exposed to medium level MW irradiation for 20 minutes.

Figure 5-4 shows the weight loss in the preparation of samples 12- 15. The results showed that the higher the microwave power was, the faster the weight loss occurred. Considering that heat was dissipated to the environment through the surface

[1] The BET surface area of F400 AC listed in this table is higher than that listed in Chapter 2. This is because the relative pressure ranges of the adsorption data used in the multipoint BET calculation were different. The relative pressure range used here was 0.005 -0.20. The relative pressure range used in Chapter 2 was 0.05 -0.30.

continuously, the bulk temperature and heating rate of the sample under different microwave power levels should be different. Although the bulk temperature wasn't measured because of the facility limitation, it can be conjectured that the bulk temperature and heating rate increased with the power level. The weight loss of sample 15 was faster than that of sample 12 although the microwave power levels used were the same. The evaporation of water and solvent was responsible for the difference. Due to the different heat capacities of these two materials, the heat dissipation rate was also different, which resulted in bulk temperature of sample 15 being higher than that of sample 12. Assuming that all the TTIP was converted into TiO_2, 0.13 g TiO_2 would be generated. The weights of sample 12-15 were 1.13 g, 1.13 g, 1.32 g and 1.10 respectively. Clearly, the low power level was not enough to vaporize the chemicals and there was still volatile material (solvent, by-products, and/or unhydrolyzed TTIP) adsorbed on sample 14. Hence, low power level was not considered in subsequent experiments. Considering the weight loss of virgin AC under microwave irradiation (0.03 g), the expected weight was 1.10. Therefore, the TTIP conversion of samples 12 and 13 perhaps were also incomplete.

The TiO_2 loading, BET surface area, and total pore volume of TiO_2/AC sample are also listed in Table 1. The ash content of F400 AC after microwave process was used to calculate the TiO_2 loading. The various preparation conditions listed in Table 5-2 did not exhibit significant influences on the TiO_2 loading, specific surface area, and total pore volume of samples 15, 16 and 17. Compared with samples 15, 16 and 17, these properties of samples 12 and 13 were lower. This further supports that the TTIP conversion of samples 12 and 13 was not complete. Compared with virgin F400 AC, however, the

specific surface area and total pore volume of samples 15 – 17 were lower which resulted from the TiO_2 deposited on the carbon surface that blocked the pores.

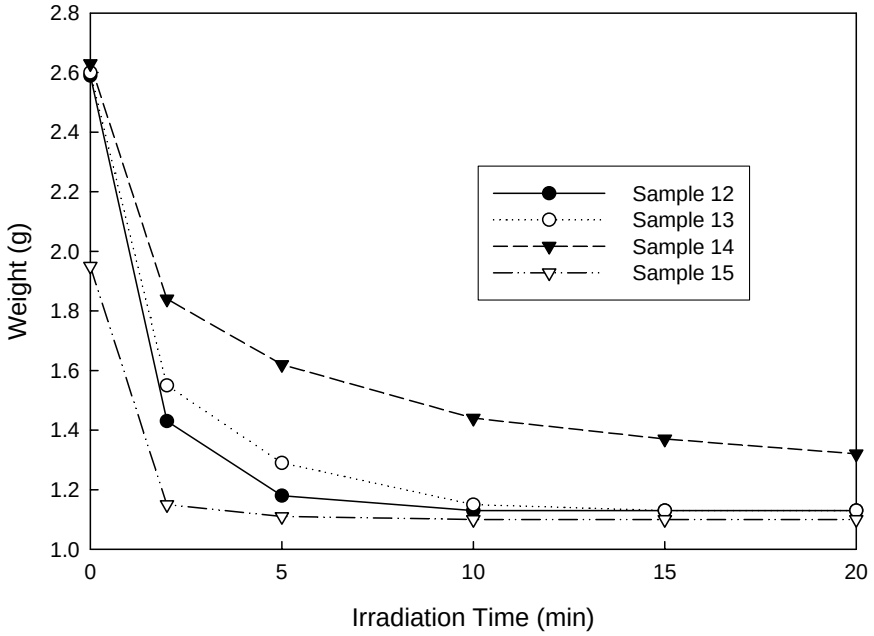

Figure 5-4 Weight loss curves of TiO_2/AC samples

TiO_2/AC Characterization

Figure 5-5 shows the SEM images of TiO_2/AC prepared by the described method and the virgin carbon. It demonstrates that TiO_2 particles were formed on the carbon surface. The preparation conditions didn't significantly affect the TiO_2 morphology because the actual power output rate at each condition was the same; just the irradiation time was changed. Figure 5-6 shows the SEM image of the cross-section of sample 12. Figure 5-7 shows the SEM images, EDS spectra, and the EDS mapping of Ti element on section 1 (external surface) and section 2 (internal surface) in Figure 5-6. Obviously, the formed TiO_2 was rich on the external surface of carbon. The deposition of TiO_2 on the external surface is preferred since UV light cannot penetrate into inner pores. Because water was added later, thermal reaction of TTIP inside pores could yield TiO_2 on the

(a)

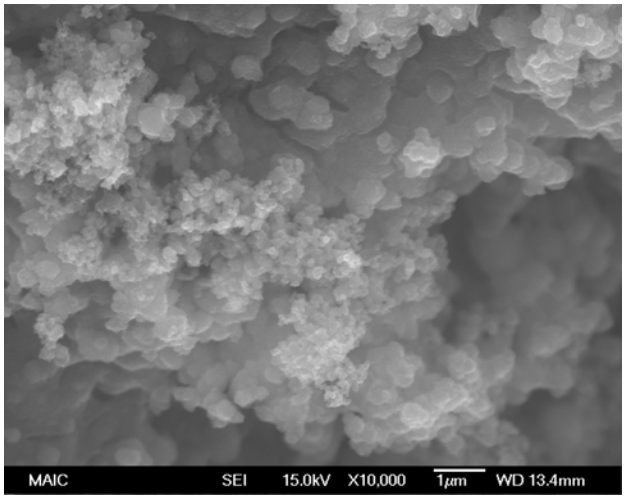

(b)

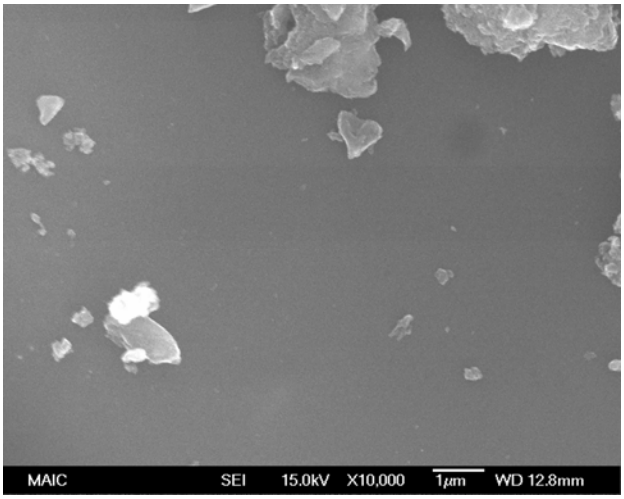

Figure 5-5 SEM images of TiO_2/AC samples: (a) Sample 15; (b) Virgin Carbon

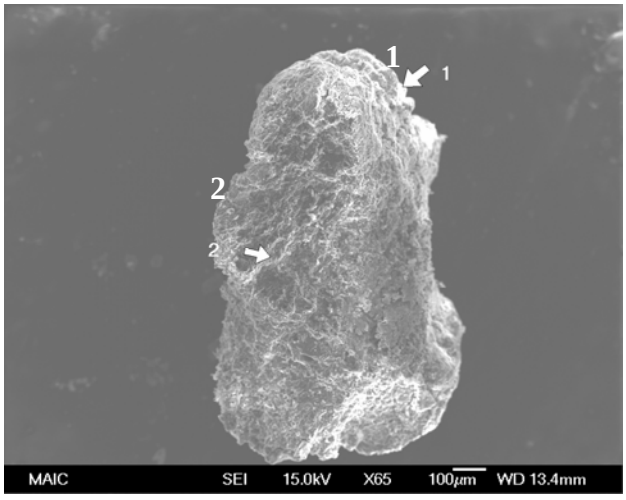

Figure 5-6 Cross-section of Sample 12

internal surface. Under microwave irradiation, however, part of TTIP inside pores could also be desorbed and/or evaporated out before decomposition. These TTIP molecules reacted with water and then deposited on outer surface.

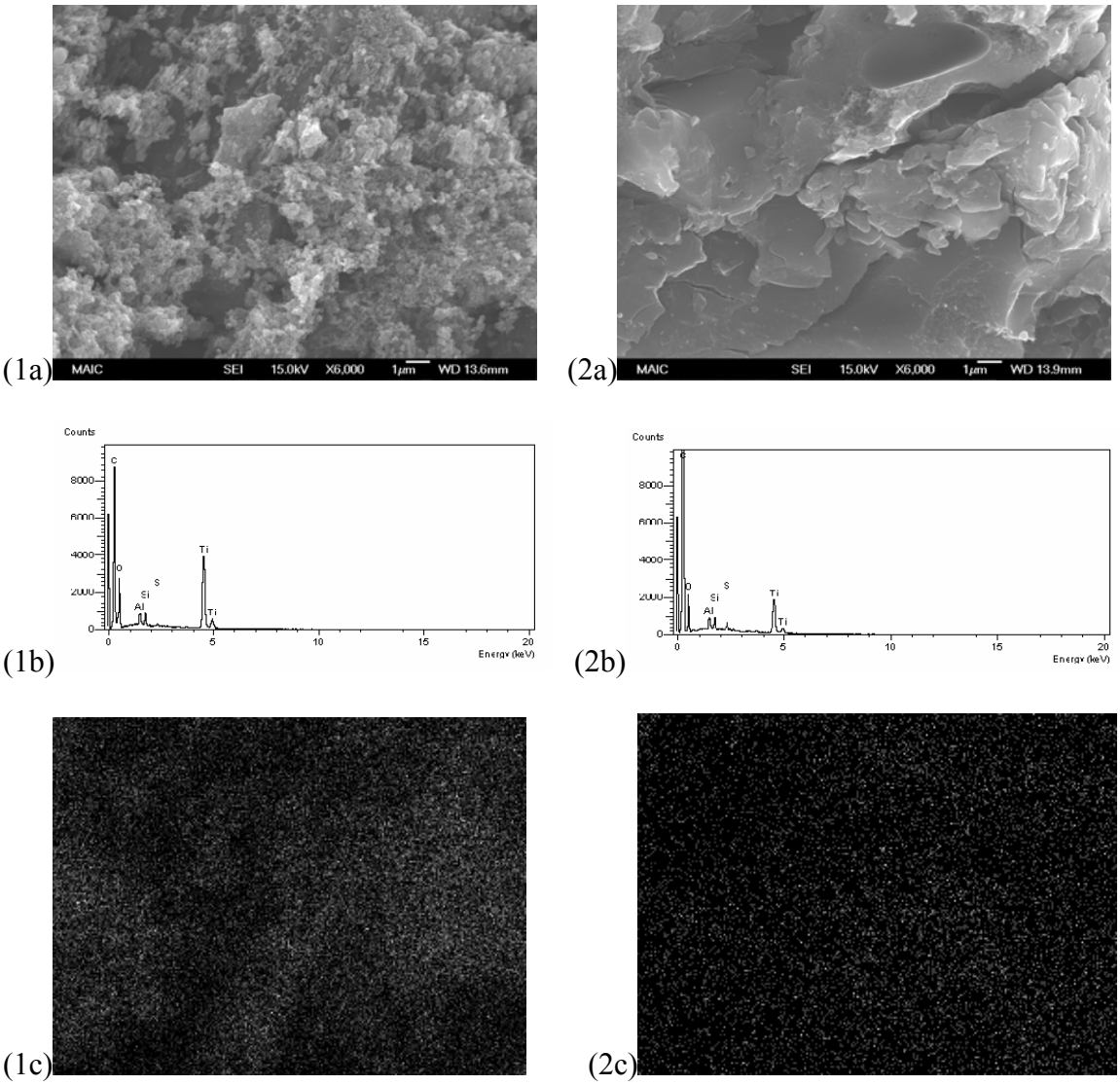

Figure 5-7 Region 1 and Region 2 in Figure 5-6: (a) SEM images; (b)EDS spectra; (c)EDS mapping of Ti element.

Figure 5-8 shows the XRD patterns of different samples. Fast scanning speed, 0.05 ^{o}/sec was used initially. If any clear peaks were detected, slow scanning speed, 0.005 ^{o}/sec was used to verify the result. No significant peak was detected on samples 12 and 13. However, some peaks were detected on samples 15 -17. Therefore slow scanning

speed was used to rerun samples 15-17. The results revealed that anatase phase was formed on samples 15 and 17, and rutile phase was formed on samples 16 and 17 that resulted from the high bulk temperature. The formation of anatase TiO_2 is important due to its photocatalytic performance, which will be explained in the next section.

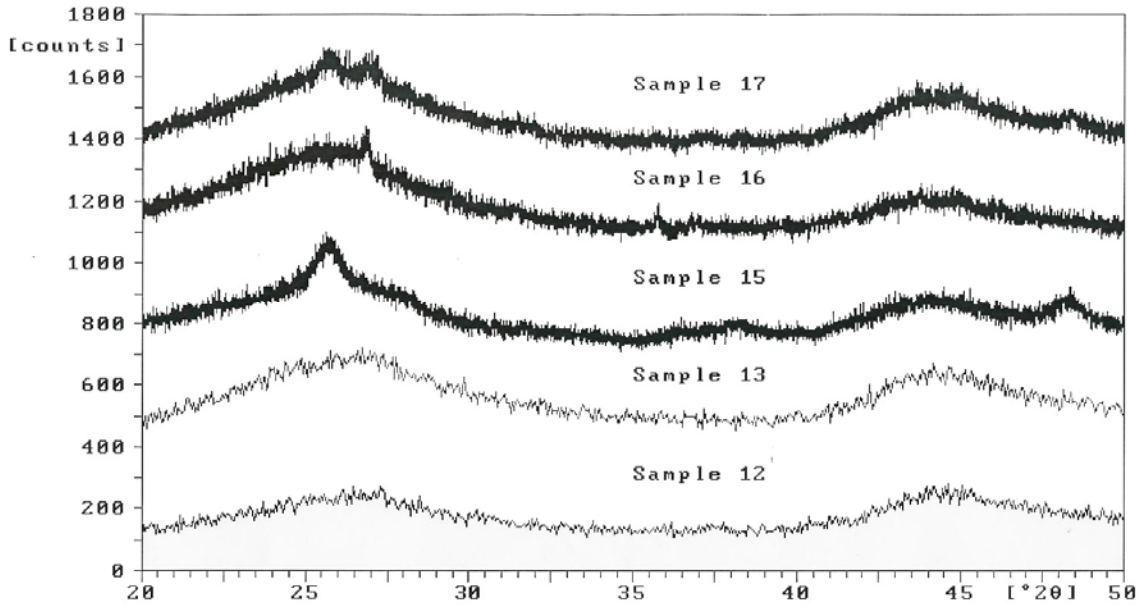

Figure 5-8 XRD patterns of different samples (scanning speed: 0.05 ^{o}/sec for samples 12 and 13; 0.005 ^{o}/sec for samples 15 -17)

Methanol removal testing

Methanol removal by the original F400 AC and TiO_2/AC composites with and without UV light was carried out in order to compare their ability. The inlet methanol concentration was 22.4 ppm. The relative effluent methanol concentration profiles for the virgin AC and TiO_2/AC are shown in Figure 5-9. It is apparent from Figure 5-9 that the effluent methanol concentration increased quickly when treated by the virgin AC with and without UV light. When treated by TiO_2/AC without UV light irradiation, a similar adsorption profile was observed, and the methanol adsorption capacities for sample 12 composite was actually lower than that of the virgin carbon due to the lower surface area.

However, with UV light irradiation, the methanol concentration did not reach saturation for the duration of the experiment. Another thing that should be mentioned was that acetone and 2-propanol were detected by GC in the impinger samples of samples 12 and 13 (with UV light). Acetone is the product of reaction between TTIP and the carbonyl groups on activated carbon surface (Tatsuda et al., 2005). Because acetone and 2-propanol weren't the products of methanol degradation, their presence further proved that the TTIP conversion of samples 12 and 13 was incomplete. Regarding sample 15 (with UV light), the effluent methanol concentration increased during the first 2 hours and then maintained at about 53% removal. Therefore, the average of the last four data was used to calculate the average methanol removal efficiency for subsequent analysis.

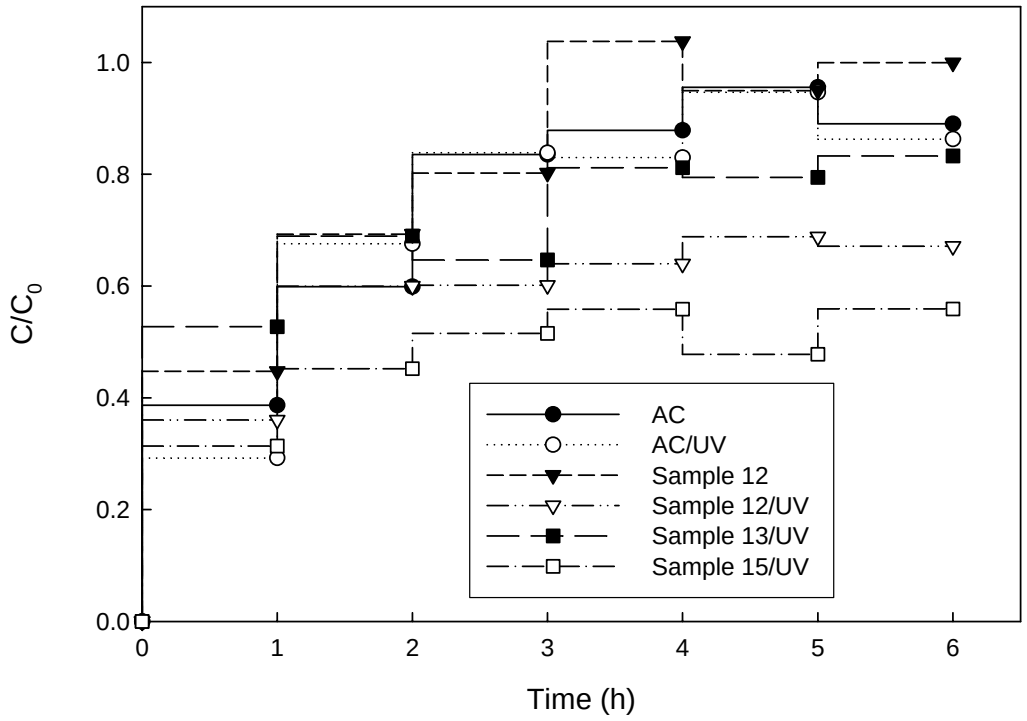

Figure 5-9 Methanol effluent concentration profiles: inlet methanol concentration was 22.4 ppm, inlet water concentration was 19 mgL^{-1}, EBCT was 0.35 s

Figure 5-10 shows the average methanol removal efficiencies of samples 15 -17 with UV irradiation. No acetone and 2-propanol were detected by GC in the impinger samples of these samples, and their average methanol removal efficiencies were similar. This revealed that increasing the irradiation time can not further increase the photocatalytic activity once the TTIP conversion was completed.

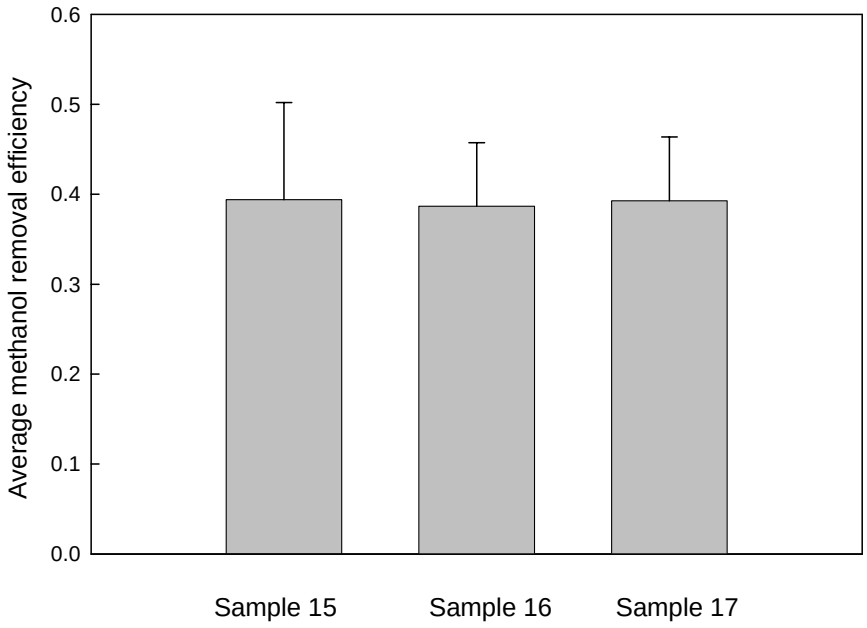

Figure 5-10 Average methanol removal efficiencies: inlet methanol concentration was 38.8 ppm, inlet water concentration was 19 mgL^{-1}, EBCT was 0.35 s

Conclusions

Under medium level of 800 W microwave irradiation, anatase TiO_2 was quickly formed from TTIP precursor in a short time, at atmospheric pressure. F400 AC was stable under this energy level, and the formed submicron TiO_2 particles were rich on the external surface of carbon. When the TTIP conversion was completed, the irradiation time and water/TTIP ratio would no longer pose any significant impact on the final product. The prepared TiO_2/AC composite photocatalyst showed lower adsorption

capacity for methanol than virgin carbon due to pore blockage by the newly formed TiO_2 particles. Photocatalytic oxidation of methanol from humid air was successfully accomplished by the composite, and the material did not reach saturation for the duration of the experiment.

CHAPTER 6
CONCLUSIONS AND RECOMMANDATIONS

Pulp and paper mills rank in the ten largest industrial activities in the United States. More and more stricter air emission regulations urged researchers and engineers to explore advanced control technologies. This study was carried out to develop TiO_2/AC composite photocatalyst as an alternative technique for the treatment of high volume low concentration air emissions from pulp and paper mills.

TiO_2/AC composite prepared by conventional methods as well as microwave methodology was characterized and evaluated by activity tests for the degradation of methanol and H_2S, two important pollutants of HVLC air emissions from pulp and paper mills.

First, the technical efficacy of photocatalytic regeneration of the spent carbon was investigated. The model pollutant, methanol, was removed from airstreams using TiO_2/AC composite prepared by spray desiccation method. The spent adsorbent was regenerated under UV light irradiation. Photocatalytic regeneration of TiO_2/AC is ascribed to both desorption from AC and photocatalytic degradation on TiO_2. Increasing desorption rate by using purge air greatly increased the regeneration capacity. However, when the desorption rate was greater than the photocatalytic oxidation rate, part of the methanol was directly desorbed without degradation. So, improving the photocatalytic degradation rate is important for the application of photocatalytic regeneration in the gas phase.

Dry impregnation was developed to improve the photocatalytic activity of TiO_2/AC composite. Titanium tetra-isopropoxide (TTIP), the precursor, was effectively converted to the anatase form of TiO_2 on the carbon surface after hydrolysis and calcination. Under proper preparation conditions, the TiO_2/AC composite outperformed the composite prepared by spray desiccation method in removing methanol. Another model pollutant, hydrogen sulfide, also photocatalytically degraded on TiO_2/AC composite. The sulfate conversion efficiency of TiO_2/AC composite was higher than that of AC. A high sulfate conversion efficiency is desired since the formed sulfate can be easily washed away.

Finally, a novel microwave-assisted impregnation was developed for TiO_2/AC composite photocatalyst preparation. Due to the volumetric heating and selective heating of microwave, the solvent and by-products were quickly removed which required less energy and shorter processing time. The formed submicron TiO_2 particles were mainly deposited on the external surface of carbon.

Based on the conclusions presented above and the experience gained in this research, recommendations can be made to help further advance the application of TiO_2/AC composite photocatalyst.

1. The moisture in carbon is beneficial to the hydrolysis of TTIP. The effect of moisture content on the performance of final product should be further studied. There will be a relationship between the moisture content and the hydrolysis degree. When the moisture reaches a critical value, it is possible that no extra water is needed for the hydrolysis of TTIP. An additional benefit is that the hydrolysis and drying can be combined into one step. However, there is a critical issue of how to control the moisture content of the carbon and its distribution to deliver optimal result.

2. The UV light (peak wavelength is 365 nm) irradiation improved the H_2S removal and sulfate conversion efficiency on virgin BioNuchar AC. The mechanism has not been reported in prior work. Two possible mechanisms can be hypothesized: 1) the adsorbed H_2S and/or the oxidation products of H_2S on AC (mainly elemental sulfur) could be excited under the irradiation of UV light which may create a more

adsorbable species; 2) the surface of AC can be modified by UV light irradiation. These hypotheses are worthy of exploration.

3. The application of the suggested microwave-assisted impregnation can be further studied. This method may be applied to preparation of supported catalyst. Due to the facility limitation, the microwave power and sample temperature couldn't be controlled. This limited further investigation of the suggested method. Inert atmosphere could be used to protect the carbon and avoid any possible combustion and explosion. Thermally insulating material, temperature sensors, and automatic power control systems could be used to improve the uniformity of microwave heating and avoid overheating. Further understanding of how microwave energy interacts with materials is the key.

4. Investigated the effect of different types of AC (coal based or wood based) on photocatalytic activity of TiO_2/AC composite.

LIST OF REFERENCES

Aikyo, H., Suzuki, M., Matsumura, A. I. K., Okuyama, K., 1996. The European Caubon Conference Carbon 96, Newcastle, UK, (Extended Abstracts), 296.

Alberici, R. M., Jardim, W. F., 1997. Photocatalytic destruction of VOCs in the gas-phase using titanium dioxide. Appl. Catal. B: Env. 14, 55-68.

Ao, C.H., Lee, S.C., 2003. Enhancement effect of TiO_2 immoblized on activated carbon filter for the photodegradation of pollutants at typical indoor air level. Appl. Catal. B: Env. 44, 191-205.

Araña, J., Doña-Rodríguez, J.M., Garriga I Cabo, C., González-Díaz, O., Herrera-Melián, J.A., Pérez-Peña, J., 2004. FTIR study of gas-phase alcohols photocatalytic degradation with TiO_2 and AC-TiO_2. Appl. Catal. B: Environ. 53, 221-232.

Ayllón. J. A., Peiró, A. M., Saadoun, L., Vigil, E., Domènech, X., Peral, J., 2000. Preparation of anatase powders from fluorine-complexed titanium (IV) aqueous solution using microwave irradiation. J. Mater. Chem. 10, 1911-1914.

Bandosz, T., 2002. On the adsorption/oxidation of hydrogen sulfide on activated carbons at ambient temperatures. J. Colloid Interface Sci. 246, 1-20.

Bargreev, A., Adib, F., Bandosz, T., 2001. pH of activated carbon surface as an indication of its suitability for H_2S removal from moisture air streams. Carbon 39, 1897-1905.

Bathen, D. Physical waves in adsorption technology-an overview. Sep. Purif. Technol. 2003, 33, 163.

Bhatkhande, D. S., Pangarkar, V. G., Beenackers A. ACM, 2001. Photocatlytic degradation for envirnmental applications – a review. J. Chem. Technol. Biotechnol. 77, 102-116.

Bordado, J. C. M., Gomes, J. F. P., 2002. Atmospheric emissions of Kraft pulp mills. Chem. Eng. Processing 41, 667-671.

Bouzaza, A., Laplanche, A., Marsteau, S., 2004. Adsorption-oxidation of hydrogen sulfide on activated carbon fibers: effect of the composition and the relative humidity of the gas phase. Chemosphere 54, 481-488.

Buonicore, A. J., Davis, W. T. Air pollution engineering manual. AWMA. Van Nostrand Reinhold, New York.

Bykov, Y. V., Rybakov, K. I., Semenov, V. E., 2001. High-temperature microwave processing of materials. J. Phys. D: Appl. Phys. 34, 55-75.

Canela, M. C., Alberici, R. M. Jardim, W. F., 1998. Gas-phase destruction of H_2S using TiO_2/UV-VIS. J. Photoch. Photobio. A: Chem. 112, 73-80.

Capio, E., Zúñiga, P., Ponce, S., Solis, J., Rodriguez, J., Estrada, W., 2005. Photocatlytic degradation of phenol TiO_2 nanocrystals supported on activated carbon. J. Mol. Catal. A 228, 293-298.

Carrott, P. J. M., Nabais, J. M. V., Ribeiro Carrott, M. M. L., Pajares, J. A., 2001. Preparation of activated carbon fibres from acrylic textile fibres. Carbon 39, 1543-1555.

Chang, C., Chen, J., Lu, M., Yang, H., 2005. Photocatalytic oxidation of gaseous DMF using thin film TiO_2 photocatalyst. Chemosphere 58, 1071-1078.

Chen, A., Lu, G., Tao, Y., Dai, Z., Gu, H.,2001. Novel photocatlyst immobilized on springs and packed bed photoreactor. Mater. Phys. Mech. 4,121-124.

Colón,G., Hidalgo, M. C., Macías, M., Navío, J. A., Doña, J. M., 2003. Influence of residual carbon on the photocatalytic activity of TiO_2/C samples for phenol oxidation. Appl. Catal. B: Environ.43,163.

Crittenden, J. C., Notthakun, S., Hand, D. W., Perram, D. L., 1993. Regeneration of adsorbents using advanced oxidation. US Patent, No. 5,182,030.

Crittenden, J. C., Suri, R. P. S., Perram, D. L., Hand, D. W., 1997. Decontamination of water using adsorption and photocatalysis. War. Res. 31, 411-418.

Degussa AG, Titanium dioxide P 25. Technical Bulletin No. 80, September 2003. Technical.service.aerosil@degussa.com

Ding, Z., Hu, X., Yue, P. L., Gao, Q. L., Greenfield, P. F., 2001. Synthesis of anatase TiO_2 supported on. Porous solids by chemical vapor deposition. Catal. Today 68, 173-182.

DOE (Department of Energy). Forest products annual report, 2003. Washington DC United States.

El-Sheikh, A. H., Newman, A. P., Al-paffaee, H., Phall, S., Cresswell, N., York, S., 2004. Deposition of anatase on the surface of activated carbon. Surf. Coat. Technol. 187, 284-292.

Finqueneisel, G., Zimny, T., Weber, J. V., 2005. On the prediction of adsorption isotherms of methanol/water vapour mixtures on microporous activated carbon. Carbon 43, 1093-1095.

Giesche, H., 1998. Preparation and applications of coated powders in ceramics and related fields. J. Disper. Sci. Technol. 19, 249 (M1)

Gubkina, M. L., Larin, A. V., Polyakov, N. S., 2003. Measurement of adsorption isotherm of methanol on a humidified activated carbon by the dynamic method. Colloid J. 65, 155-158.

Harada, M., Honda, M., Yamashita, H., Anpo, M., 1999. preparation of titanium oxide photocatalysts loaded on activated carbon and their photocatalytic reactivity for the degradation of 2-propanol diluted in water. Res. Chem. Intermed. 25, 757-768.

Hart, J. N., Cervini, R. Cheng, Y.-B., Simon, G.P., Spiccia, L., 2004. Formation of anatase TiO_2 by microwave processing. Sol. Energy Mater. Sol. cells 84, 135-143.

Hayes, B. L., 2002. Microwave Synthesis: Chemistry at the Speed of Light, CEM Publishing: Matthews, NC.

Herrmann, Jean-Marie, Guillard, Chantal. 2000, Photocatalytic degradation of pesticides in agricultural used waters. Comptes Rendus de l'Academie des Sciences, Serie IIc: Chimie C.R.Acad. Sci. Paris, Serie IIc, Chimie 3, 417-422.

Hoffmann, M. R., Martin, S. T., Choi, W., Bahnemann, D. W., 1995. Environmental applications of semiconductor photocatalysis. Chem. Rev. 95, 69-96.

Huang, Z., Zhu, Z., Liu, Z., 2002. Combined effect of H_2O and SO_2 and V_2O_5/AC catalysts for NO reduction with ammonia at Lower Temperatures. Appl. Catal. B: Environ. 39, 361.

Jeong, J., Sekiguchi, K., Sakamoto, K., 2004. Phtochemical and photocatalytic degradation of gaseous toluene using short-wavelength UV irradiation with TiO_2 catalyst: comparison of three UV sources. Chemosphere 57, 663-671.

Khan, A. M., 2003. Titanium Dioxide Coated Activated Carbon: A Regenerative Technology for Water Recovery. Master's Thesis, University of Florida.

Khan, A.Y., Mazyck, D. W., Wu, C., 2002. TiO_2 coated activated carbon: a regenerative technology for water recovery. NAA ICE Conference.

Khriachtchev, L., Pettersson, M., Isoniemi, E., Räsänen, M., 1998. 193 nm photolysis of H_2S in rare-gas matrices: Luminescence spectroscopy of the product. J. Chem. Phys. 108, 5747- 5754.

Kim, J. S., Ki C., Pratsinis, S. E., 2000. The effect of hydrolysis temperature on the synthesis of bimodally nanostructured porous titania. J. Nanopart. Res. 2, 419.

Kim, S. B., Hong, A. C., 2002. Kinetic study for photocatalytic degradation of volatile organic compounds in air using thin film TiO_2 photocatalyts. Appl. Catal. B: Env. 35, 305-315.

Kirkbir, K. and Komiyama, H., 1998. Continuous production of fine TiO_2 powder by vapor-phase hydrolysis of titanium tetraisopropoxide. Adv. Ceram. Mater. 3, 511.

Kong, Y., Cha, C.Y., 1996. Reduction of NO_x adsorption on char with microwave energy. Carbon 34, 1027.

Le Leuch, L., Subrenat, A., Le Cloirec, P., 2003. Hydrogen sulfide adsorption and oxidation onto activated carbon cloths: application to odorous gaseous emission treatment. Langmuir 19, 10869-10877.

Lee, D.K., Kim, S.C., Kim, S.J., Chung, I.S., Kim, S.W., 2004. Photocatalytic oxidation of microcystin-LR with TiO_2-loaded activated carbon. Chem. Eng. J. 102, 93-98.

Lei, L., Chu, H. P., Hu, X., Yue, P.,1999. Preparation of heterogeneous photocatalyst (TiO_2/Alumina) by metallo-organic chemical vapor deposition. Ind. Eng. Chem. Res. 38, 3381-3385.

Li, Y. H., Lee, C. W., Gullet, B.K., 2003. Importance of activated carbon's oxygen surface functional groups on elemental mercury adsorption. Fuel 82, 451-457.

Linsebigler, A. L., Lu, G., Yates, J. T., 1995. Photocatalysis on TiO_2 surfces: principles, mechanusms, and selected results. Chem. Rev. 95, 735-758.

Liu, J., Crittenden, J. C., Hand, D. W., Perram, D. L., 1996. Regeneration of adsorbents using heterogeneous photocatalytic oxidation. J. Environ. Eng. 8, 707-713.

Liu, S. X., Sun, G. L., Zhang, S. R., 2004. Photocatalytic regeneration of exhausted activated carbon saturated with phenol. Bull. Environ. Contam. Toxicol. 73, 1017-1024.

Lu, M., Chen, J., Chang, K., 1999. Effect of adsorbents coated with titanium dioxide on the photocatalytic degradation of propoxur. Chemosphere 38, 617-627.

Malato, S., Blanco, J., Fernández-lbáñez, P., Cáceres, J., 2001. Treatment of 2,4-dichlorophenol by solar photocatalysis: comparison of coupled photocatalytic-active carbon vs. active carbon. Trans. ASME 123, 138-142.

Matos, J., Laine, J., Herrmann, J.-M. 2001 Effect of the type of activated carbons on the photocatalytic degradation of aqueous organic pollutants by UV-irradiated titania. J. Catal. 200, 10-20.

Mergel, D., Buschendorf, D., Eggert, S., Grammes, R. And Samset, B., 2000. Thin Solid Films, 371, 218.

NCASI (National Council of Air and Stream Improvement) Method CI/SG/PULP-94.02., 1998NCASI Southern Regional Center.

NCASI (National Council of Air and Stream Improvement) Technical Bulletin No. 676, 1994. Volatile organic emission from pulp and paper mill sources part II – lime kilns, smelt dissolving tanks and miscellaneous causticizing area vent. New York, N.Y.:

Noll, K. E., 1999. Fundamentals of air quality systems: design of air o\pollution control devices. American Academy of Environmental Engineers, Annapolis, MD.

Nozawa, M., Tanigawa, K., Hosomi, M., Chikusa, T., Kawada, E., 2001. Removal and decomposition of malodorants by using titanium dioxide photocatalyst supported on fiber activated carbon. Water Sci. Technol. 144, 127-133.

Peral J, Domènech X, Ollis D, 1997. Heterogeneous photocatalysis for purification, decomtamination and deodorization of air. J. Chem.. Technol. Biotechnol. 70, 117-140.

Perego, C., Villa, P., 1997. Catalyst preparation methods. Catal. Today 34, 281.

Petre, C., Larachi, F., 2005. Bifunctional redox iron/cerium (hydr)oxide process for H_2S removal from pulp and paper emissions. Ind. Eng. Chem. Res. 44, 9391-9397.

Pitoniak, E., Wu, C.-Y., Londeree, D., Mazyck, D., Bonzongo, J.-C., Powers, K., Sigmund, W., 2003. Nanostructured Silica-Gel Doped with TiO2 for Mercury Vapor Control. J. Nanopa. Res. 5, 281-292.

Pozzo, R. L., Giombi, J. L., Baltanás, M. A., Cassano, A. E., 2000.The performance in a fluidized bed reactor of photocatalyst immobilized onto inert supports. Catal. Today 62, 175.

Przepiorski, J., Yoshizawa, N., Yamada, Y., 2001. Activated carbons containing TiO2: characterization and influence of a preparation method on the state of supported TiO_2. J. Mater. Sci. 36, 4249.

Qourzal, S., Assabbane, A., Ait-Ichou, Y., 2004. Synthesis of TiO_2 via hydrolysis of titanium tetraisopropoxide and its photocatalytic activity on a suspended mixture with activated carbon in the degradation of 2-naphthol. J. Photoch. Photobio. A: Chem. 16, 317.

Ramakrishnan, K. N., 1999. Powder particle size relationship in microwave synthesized ceramic powders. Mater. Sci. Eng. 259, 120-125.

Rubio,F., Rubio, J., Duran, P., Oteo, J. L., 1999. Preparation of nanometric titanium hydrous oxide particles by vapor phase hydrolysis of titanium tetrabutoxide. J. Mater. Sci. 34, 3397.

Sadeghi, M., Liu, W., Zhang, T., Stavropoulos, P., Levy, B., 1996. Role of photoinduced charged carrier separation distance in heterogeneous photocatalysis: oxidation degradation of CH_3OH vapor in cantact wit Pt/TiO_2 and cofumed TiO_2-Fe_2O_3. J. Phys. Chem., 100, 19466-19474.

Serros, M., 1996.Environmental fate and effects of pulp and paper mill effluent. Delray Beach, Fla.: St. Lucie Press.,

Seto, T., Shimada. M. and Okuyama, K., 1995. Evaluation of sintering of nanometer-sized titanium using aerosol method. Aerosp. Sci. Technol. 23, 183.

Sheintuch, M., Matatov-Meytal, Y. I., 1999. Comparison of catalytic processes with other regeneration methods of activated carbon. Catal. Today 53, 73-80.

Sittig, M., 1977. Pulp and paper manufacture: energy conservation and pollution prevention. Park Ridge, N.J. : Noyes Data Corp.

Sontheimer, J., Crittenden, J. C., and Summers, R. S., 1988.Activated Carbon for Water Treatment. 2nd Ed. DVGW-Forschungsstelle, Karlsruhe, Germany.

Springer, A. M., 2000. Industrial Environmental Control: Pulp and Paper Industry. TAPPI Press, Altanta, GA.

Stokke, J. M., 2003. Gas-Phase Separation of Volatile Organic Compounds Emitted from the Wood Processing Industry. Bachelor Thesis, University of Florida.

Suri, R. P. S., Liu, J., Crittenden, J. C., Hand, D. W., 1999. Removal and destruction of organic contaminants in water using adsorption, steam regeneration, and photocatalytic oxidation: a pilot-scale study. J. Air & Waste Manage. Assoc. 49, 951-958.

Sutton, W. H., Brooks, M. H., Chabnsky, I. J., 1998. Microwave processing of materials. Materials Research Society, Pittsburgh, Pennsylvania. Volume 124.

Takeda, N., Ohtani, M., Torimoto, T., Kuwabata, S., Yoneyama, H., 1997. Evaluation of diffusibility of adsorbed propionaldehyde on titanium dioxide-loaded adsorbent photocatalyst flims from its photodecomposition rate. J. Phys. Chem. B 101. 2644-2649.

Tao, Y., Schwartz, S., Wu, C.-Y., Mazyck, D. W., 2005. Development of a TiO_2/AC composite photocatalyst by dry impregnation for the treatment of methanol in humid airstreams. Ind. Eng. Chem. Res. 44, 7366-7372.

Taqvi, S. M., Scot Appel, W., Douglas Levan, M., 1999. Coadsorption of organic compounds and water vapor on BPL activated carbon. 4. Methanol, ethanol, propanol, butanol, and modeling. Ind. Eng. Chem. Res. 38, 240-250.

Tatsuda, N., Itahara, H., Setayama, N., Fukushima, Y., 2005. Preparation of titanium dioxide/activated carbon composites using supercritical carbon dioxide. Carbon, 43, 2358-2365.

Torimoto, T., Okawa, Y., Takada, N., Yoneyama, H., 1997. Effect of AC content in TiO_2-loaded AC on photodegradation behavior of dichloromethane. J. Photochem. Photobiol, A: chem, 103, 153-157.

Ubuka, T., Abe, T., Kajikawa, T., Morino, K., 2001. J. Chromatogr., B: Anal. Technol. Biomed. Life Sci. 757, 31.

Varma, V. K., 2003. Experience with the collection, transport, and burning of kraft mill high volume low concentration gases. NCASI Special Report No. 03-03.

Wilson, G. J., Will, G.D., Frost, R. L., Montgomery, S.A., 2002. Efficient microwave hydrothermal preparation of nanocrystalline anatase TiO_2 colloids. J. Mater. Chem. 12, 1787-1791.

Wu, CY, Lee, TG, Tyree, G., Arar, E., Biswas, P., 1998. Capture of mercury in combustion systems by in situ generated titania particles with UV irradiation. Env. Eng. Sci. 15, 137-148.

Yamamoto, T., Wada, Y., Yin, H., Sakata, T., Mori, H., Yanagida, S., 2002. Microwave-driven polyol method for preparation of TiO_2 nanocrystallites. Chem. Lett. 964-965.

Yamashita, H., Harada, M., Tanii, A., Honda, M., Takeuchi, M., Ichihashi, Y., Anpo, M., Iwamoto, N., Itoh, N., Hirao, T., 2000. Preparation of efficient titanium oxide photocatalysts by an ionized cluster beam (ICB) method and their photocatalytic reactivities for the purification of water. Catal. Today 63, 63-69.

Yang, Y.,1992. Biofiltration for control of hydrogen sulfide. Ph.D.dissertation, University of Florida.

Yoneyama, H., Torimoto, T., 2000. Titanium dioxide/adsorbent hybrid photocatalysts for photodestruction of organic substances of dilute concentrations. Catal. Today 58, 133.

BIOGRAPHICAL SKETCH

Yong Tao was born in Shijiazhuang, Hebei province, P. R. China, on June 19, 1975. She graduated from Shijiazhuang No. 23 high school in 1993 and went to East China University of Science and Technology in Shanghai in the same year. She applied to the Biochemistry Department but she was admitted to the Inorganic Materials Department. After she got her Bachelor of Engineering degree from Inorganic Materials Department in 1997, she worked in Shanghai Huaming Hi-Tech (group) Co. Ltd. for one year. Influenced by her twin sister, Hui Tao, She attended the National Graduate School Entrance Exam in January 1998 and was admitted to Chemical Engineering Department of East China University of Science and Technology. After graduating with Master of Engineering degree in 2001, she worked as the application lab manager in NETZSCH instruments (Shanghai) Co. Ltd. Then she decided to pursue her Ph.D. degree in USA. In 2003, she was admitted with a research assistantship from Dr. Chang-Yu Wu to Environmental Engineering and Sciences Department in University of Florida and started her Ph.D. study.